Inorganic Chemistry

ARTICLE

pubs.acs.org/IC

Synthesis, Structure, and Reactivity of New Tetranuclear Ru-Hbpp-Based Water-Oxidation Catalysts

Laia Francàs,[†] Xavier Sala,[†] Eduardo Escudero-Adán,[‡] Jordi Benet-Buchholz,[‡] Lluís Escriche,*[,†] and Antoni Llobet*[,†,‡]

[†]Departament de Química, Universitat Autònoma de Barcelona, Cerdanyola del Vallès, E-08193 Barcelona, Spain

[‡]Institute of Chemical Research of Catalonia, Avinguda Països Catalans 16, E-43007 Tarragona, Spain

Supporting Information

ABSTRACT: The preparation of three new octadentate tetranucleating ligands made out of two Ru-Hbpp-based units [where Hbpp is 3,5(bispyridyl)pyrazole], linked by a xylyl group attached at the pyrazolate moiety, of general formula $(Hbpp)_2$-*u*-xyl (*u* = *p*, *m*, or *o*) is reported, together with its dinucleating counterpart substituted at the same position with a benzyl group, Hbpp-bz. All of these ligands have been characterized with the usual analytical and spectroscopic techniques. The corresponding tetranuclear ruthenium complexes of general formula $\{[Ru_2(trpy)_2(L)]_2(\mu\text{-}(bpp)_2\text{-}u\text{-xyl})\}^{n+}$ [L = Cl or OAc, *n* = 4; L = $(H_2O)_2$, *n* = 6] and their dinuclear homologues $\{[Ru_2(trpy)_2(L)](\mu\text{-bpp-bz})\}^{n+}$ [L = Cl or OAc, *n* = 2; L = $(H_2O)_2$, *n* = 3] have also been prepared and thoroughly characterized both in solution and in the solid state. In solution, all of the complexes have been characterized spectroscopically by UV−vis and NMR and their redox properties investigated by means of cyclic voltammetry techniques. In the solid state, monocrystal X-ray diffraction analysis has been carried out for two dinuclear complexes $\{[Ru_2(trpy)_2(L)](\mu\text{-bpp-bz})\}^{2+}$ (L = Cl and OAc) and for the tetranuclear complex $\{[Ru_2(trpy)_2(\mu\text{-OAc})]_2(\mu\text{-}(bpp)_2\text{-}m\text{-xyl})\}^{4+}$. The capacity of the tetranuclear aqua complexes $\{[Ru_2(trpy)_2(H_2O)_2]_2(\mu\text{-}(bpp)_2\text{-}u\text{-xyl})\}^{6+}$ and the dinuclear homologue $\{[Ru_2(trpy)_2(H_2O)_2](\mu\text{-bpp-bz})\}^{3+}$ to act as water-oxidation catalysts has been evaluated using cerium(IV) as the chemical oxidant in pH = 1.0 triflic acid solutions. It is found that these complexes, besides generating significant amounts of dioxygen, also generate carbon dioxide. The relative ratio of $[O_2]/[CO_2]$ is dependent not only on para, meta, or ortho substitution of the xylylic group but also on the concentration of the starting materials. With regard to the tetranuclear complexes, the one that contains the more sterically constrained ortho-substituted ligand generates the highest $[O_2]/[CO_2]$ ratio.

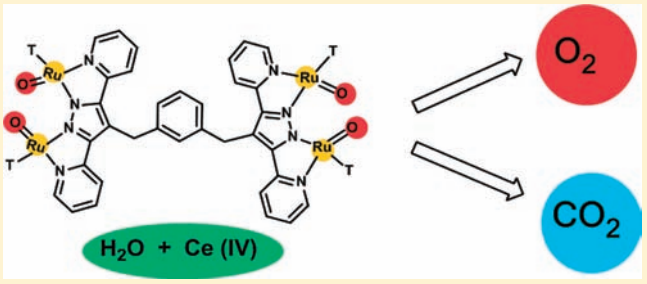

INTRODUCTION

The oxidation of water into molecular oxygen is of particular interest because it is one of the key reactions involved in solar energy conversion schemes.[1] At the moment, there are a significant number of molecular transition-metal complexes that have shown activity with regard to the oxidation of water to oxygen,[2−4] mainly based on ruthenium but also containing other metals such as iridium,[5] cobalt,[6] iron,[7] or manganese.[8]

Elucidation of the mechanism(s) by which such water-oxidation reactions occur still remains an important challenge given the molecular complexity of this reaction, which is illustrated as

$$2H_2O \rightarrow O_2 + 4H^+ + 4e^- \quad (E = 1.23\ \text{V vs NHE at pH} = 0) \qquad (1)$$

and involves the removal of four protons and four electrons from two water molecules and the formation of an O−O double bond. Furthermore, the understanding of the different parameters that influence a catalysts performance, including those exerted by auxiliary ligands, is of paramount importance in order to deepen our knowledge and further progress in this field.

The water oxidation to molecular oxygen is also of interest from a bioinorganic perspective because this is the reaction that takes place in the dark for OEC-PSII.[9] Low-molecular-weight functional models are valuable in order to shed some light on the potential mechanisms that can take place at the natural site.

We have reported the structure and spectroscopic properties of the dinuclear Ru-Hbpp water-oxidation catalyst (WOC)[10] $\{[Ru^{II}(trpy)(H_2O)]_2(\mu\text{-bpp})\}^{3+}$ ($\mathbf{3}^{3+}$), which contains the auxiliary ligands 2,2′:6′,2″-terpyridine (trpy) and 3,5-bis(pyridyl)pyrazolate (bpp), and have studied its reactivity and established its reaction mechanism.[11] Recently, it has been reported that mononuclear ruthenium complexes such as $[Ru(T)(B)(OH_2)]^{2+}$ (T is a tridentate meridional ligand such as trpy and substituted trpys or 2,6-bis(1-methylbenzimidazol-2-yl)pyridine; B is a bidentate chelating ligand such as 2,2′-bpy or substituted bpy, 2,2′-bipyrimidine or 2,2′-bipyrazine),[12,13] are efficient WOCs. However, their dinuclear counterparts bridged by two methylenic bridges such as $\{[Ru(trpy)(OH_2)]_2(\mu\text{-bbpy})\}^{4+}$ [bbpy is 1,2-bis(5′-methyl-2,2′-bipyridin-5-yl)ethane; see Chart 1 for a

Received: September 2, 2010
Published: March 02, 2011

Chart 1. The Ligands

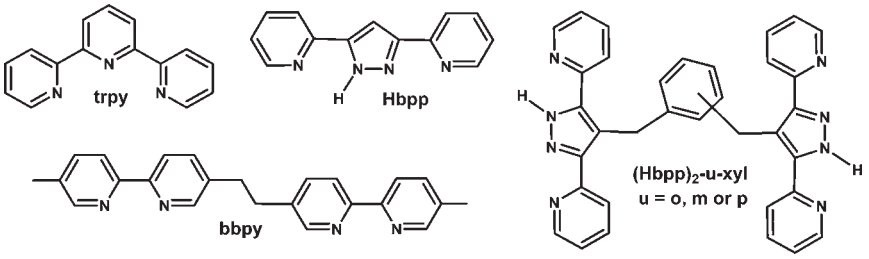

Scheme 1. Ligand Synthesis Strategy

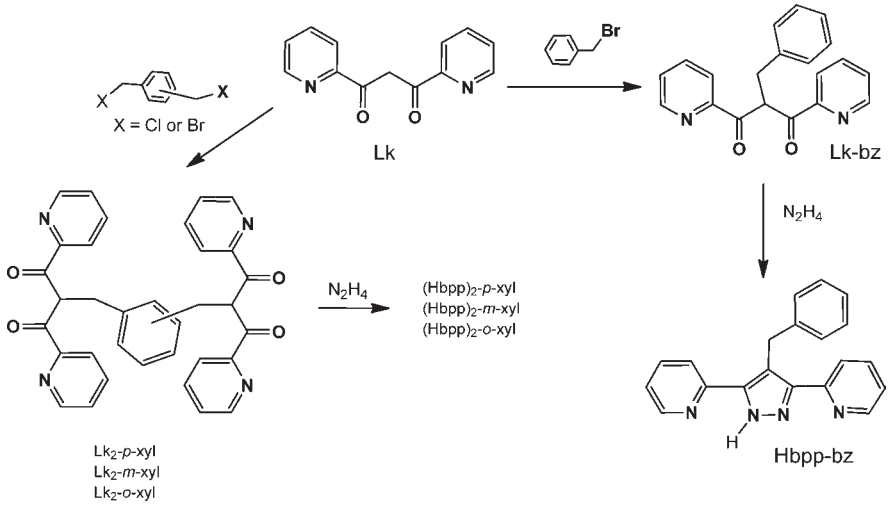

drawing of this ligand) drastically decrease their activity by nearly a third with regard to the mononuclear complex for reasons that are not well understood.[14] Given this surprising result, we wanted to check whether this is a general effect for the ruthenium WOCs and also try to understand its origin. For this purpose, we have prepared, isolated, and thoroughly characterized a family of tetranuclear ruthenium complexes containing tetranucleating ligands [$(Hbpp)_2$-*u*-xyl; *u* = *p*, *m*, or *o*] made out of two dinucleating Hbpp-based units linked by a xylyl group bonded to the pyrazolate group, as shown in the drawing in Chart 1. Meta, para, or ortho substitution of the xylyl group generates a dimer of dimers type of complex with different relative spatial dispositions of the two dinuclear subunits. From here on, we present the redox chemistry related to tetranuclear complexes of general formula $\{[Ru_2(trpy)_2(L)]_2(\mu\text{-}(bpp)_2\text{-}u\text{-xyl})\}^{n+}$ [L = Cl or OAc, *n* = 4; L = $(H_2O)_2$, *n* = 6] and their dinuclear homologues $\{[Ru_2(trpy)_2(L)](\mu\text{-bpp-bz})\}^{n+}$ [L = Cl or OAc, *n* = 2; L = $(H_2O)_2$, *n* = 3; bpp-bz is the benzyl-Hbpp ligand drawn in Scheme 1]. Further, their capacity to oxidize water to dioxygen has been studied and rationalized.

EXPERIMENTAL SECTION

Materials. All reagents used in the present work were obtained from Aldrich Chemical Co. and were used without further purification. Reagent-grade organic solvents were obtained from SDS. $RuCl_3 \cdot 3H_2O$ was supplied by Alfa Aesar and was used as received.

Preparations. 1,3-Bis(2′-pyridyl)-1,3-propandione (Lk),[15] 2-benzyl-1,3-dipyridin-2-ylpropane-1,3-dione (Lk-bz),[16] the Hbpp-bz ligand (Scheme 1), and the starting complex $[RuCl_3(trpy)]$[17] were prepared as previously described in the literature. All synthetic manipulations were routinely performed under a nitrogen atmosphere using Schlenk tubes and vacuum-line techniques.

2,2′-[1,4-Phenylenebis(methylene)]bis(1,3-dipyridin-2-ylpropane-1,3-dione) [***2a***; *Lk_2-p-xyl*]. A sample of 0.385 g of α,α′-dichloro-*p*-xylene (2.2 mmol), 0.240 g (6 mmol) of NaOH, 0.250 g (1.5 mmol) of KI, and 1 g (4.4 mmol) of Lk was dissolved in a CH_3CN (100 mL)/CH_2Cl_2 (15 mL) mixture. The solution was refluxed with stirring for 12 h and then filtered through Celite to remove the inorganic salts. The organic layer was evaporated to dryness under vacuum. The resulting residue was purified by column chromatography on silica gel using $CHCl_3$ as the eluent to afford **2a** as the second fraction. Yield: 0.33 g (30%).

2,2′-[1,3-Phenylenebis(methylene)]bis(1,3-dipyridin-2-ylpropane-1,3-dione) [***2b***; *Lk_2-m-xyl*]. This compound was prepared in a manner analogous to that of product **2a** but using α,α′-dichloro-*m*-xylene as the starting material. Yield: 0.43 g (35%).

2,2′-[1,2-Phenylenebis(methylene)]bis(1,3-dipyridin-2-ylpropane-1,3-dione) [***2c***; *Lk_2-o-xyl*]. A sample of 1.160 g of α,α′-dibromo-*o*-xylene (4.4 mmol), 0.480 g (12 mmol) of NaOH, 0.50 g (4 mmol) of KI, and 2.260 g (10 mmol) of Lk was dissolved in a CH_3CN (150 mL)/CH_2Cl_2 (23 mL) mixture. The solution was heated at 80 °C with stirring for 12 h. The clean-up procedure was analogous to that employed to obtain **2a**. Yield: 1.4 g (24%).

General Synthetic Procedure for $Hbpp_2$-*u*-xyl Ligands 3a, 3b, and 3c. To a flask fitted with a reflux condenser containing a mixture EtOH (50 mL) and THF (50 mL) were successively added Lk_2-*u*-xyl (0.33 mmol) and N_2H_4 monohydrate (174.5 μL). The mixture was refluxed for 7 h; during this period, a white solid precipitated from the solution. Then the white solid was filtered and dried. Yields and characterizations are given below.

dx.doi.org/10.1021/ic101802y |*Inorg. Chem.* 2011, 50, 2771–2781

*1,4-Bis[(3,5-dipyridin-2-yl-1H-pyrazol-4-yl)methyl]benzene [**3a**; (Hbpp)$_2$-p-xyl]*. Yield: 108 mg (60%). Elem anal. Calcd for ($C_{34}H_{26}N_8$): C, 74.71; H, 4.79; N, 20.50. Found: C, 73.76; H, 4.70; N, 19.89. ^{1}H NMR (400 MHz, D_2O/CF_3COOD): δ 8.73 (ddd, 4 H, $^3J_{14-13}$ = 5.94 Hz, $^4J_{14-12}$ = 1.57 Hz, $^5J_{14-11}$ = 0.56 Hz, H14), 8.42 (td, 4 H, $^3J_{12-11,13}$ = 8.05 Hz, $^4J_{12-14}$ = 1.57 Hz, 12H), 7.93 (ddd, 4 H, $^3J_{13-12}$ = 8.05 Hz, $^3J_{13-14}$ = 5.94 Hz, $^4J_{13-11}$ = 1.20 Hz, H13), 7.86 (ddd, 4 H, $^3J_{11-12}$ = 8.05 Hz, $^4J_{11-13}$ = 1.20 Hz, $^5J_{11-14}$ = 0.56 Hz, H11), 6.74 (s, 4 H, H2, H3, H5, H6), 4.10 (s, 4 H, H7). ^{13}C{^{1}H} NMR (100.6 MHz, D_2O/CF_3COOD): δ 147.77 (C12), 142.90 (C14), 142.59 (C10), 139.20 (C9), 136.69 (C1, C4), 128.91 (C2, C3, C5, C6), 127.21 (C13), 127.12 (C11), 121.59 (C8), 28.30 (C7). ESI-MS (MeOH): *m*/*z* 546.6, 547.6 ([M + H$^+$]$^+$).

*1,3-Bis[(3,5-dipyridin-2-yl-1H-pyrazol-4-yl)methyl]benzene [**3b**; (Hbpp)$_2$-m-xyl]*. Yield: 56 mg (31%). Elem anal. Calcd for ($C_{34}H_{26}N_8$): C, 74.7; H, 4.8; N, 20.5. Found: C, 74.9; H, 4.9; N, 20.1. ^{1}H NMR (360 MHz, D_2O/CF_3COOD): δ 8.65 (ddd, 4 H, $^3J_{14-13}$ = 5.93 Hz, $^4J_{14-12}$ = 1.63 Hz, $^5J_{14-11}$ = 0.75 Hz, H14), 8.35 (td, 4 H, $^3J_{12-13,11}$ = 8.05 Hz, $^4J_{12-14}$ = 1.63 Hz), 7.87 (ddd, 4 H, $^3J_{13-12}$ = 8.05 Hz, $^3J_{13-14}$ = 5.93 Hz, $^4J_{13-11}$ = 1.27 Hz, H13), 7.75 (ddd, 4 H, $^3J_{11-12}$ = 8.05 Hz, $^4J_{11-13}$ = 1.27 Hz, $^5J_{11-14}$ = 0.75 Hz, H11), 6.86 (t, 1 H, $^3J_{3-4,2}$ = 7.80 Hz, H3), 6.68 (d, 2 H, $^3J_{4-3}$ = 7.80 Hz, H4, H2), 6.49 (s, 1 H, H6), 4.05 (s, 4 H, H7). ^{13}C{^{1}H} NMR (90.5 MHz, D_2O/CF_3COOD): δ 148.63 (C12), 143.68 (C14), 143.31 (C10), 139.97 (C9), 139.44 (C1), 130.97 (C3), 128.94 (C6), 128.22 (C4, C2), 128.14 (C11), 128.08 (C13), 122.55 (C8), 29.38 (C7). ESI-MS (MeOH): *m*/*z* 546.6, 547.2 ([M + H$^+$]$^+$).

*1,2-Bis[(3,5-dipyridin-2-yl-1H-pyrazol-4-yl)methyl]benzene [**3c**; (Hbpp)$_2$-o-xyl]*. Yield: 43 mg (24%). Elem anal. Calcd for ($C_{34}H_{26}N_8$): C, 74.71; H, 4.79; N, 20.50. Found: C, 73.58; H, 5.09; N, 19.25. ^{1}H NMR (400 MHz, D_2O/CF_3COOD): δ 8.72 (dd, 4H, $^3J_{14-13}$ = 5.92 Hz, $^4J_{14-12}$ = 1.22 Hz, H14), 8.34 (td, 4 H, $^3J_{12-13,11}$ = 8.02 Hz, $^4J_{12-14}$ = 1.22 Hz, H12), 7.92 (ddd, 4 H, $^3J_{13-12}$ = 8.02 Hz, $^3J_{13-14}$ = 5.92 Hz, $^4J_{13-11}$ = 0.95 Hz, H13), 7.64 (d, 4 H, $^3J_{11-12}$ = 8.02 Hz, H11), 6.92 (dd, 2 H, $^3J_{2-3}$ = 5.78 Hz, $^4J_{2-4}$ = 3.58 Hz, H2, H5), 6.77 (dd, 2 H, $^3J_{3-4}$ = 5.78 Hz, $^4J_{3-5}$ = 3.58 Hz, H3, H4), 4.06 (s, 4 H, H7). ^{13}C{^{1}H} NMR (100.6 MHz, D_2O/CF_3COOD): δ 148.82 (C12), 144.28 (C14), 143.70 (C10), 140.52 (C9), 136.57 (C8), 130.26 (C3, C4), 130.03 (C2, C5), 128.62 (C13), 127.83 (C11), 121.63 (C1, C6), 28.02 (C7). ESI-MS (MeOH): *m*/*z* 546.6, 547.2 ([M + H$^+$]$^+$).

General Synthetic Procedure for Complexes 4(PF$_6$)$_2$, 7(PF$_6$)$_4$, 8(PF$_6$)$_4$, and 9(PF$_6$)$_4$. A sample of 0.214 g (0.485 mmol) of [$RuCl_3$(trpy)] and 61.7 mg (1.455 mmol) of LiCl was dissolved in dried MeOH (20 mL) containing 135.5 μL (0.97 mmol) of NEt_3. The mixture was stirred at room temperature for 20 min, and then dried MeOH (6 mL) containing bpp-bz$^-$ (0.2445 mmol) or (bpp)$_2$-*u*-xyl^{2-} (0.489 mmol) was added. Deprotonation was performed by the addition of a stoichiometric amount of 0.207 M MeONa. The resulting solution was heated at reflux for 4 h in the dinuclear case and overnight for the tetranuclear case and then stirred in the presence of a 100 W tungsten lamp for 12 h. The resulting solution was filtered, and a saturated NH_4PF_6 aqueous solution (1 mL) and water (3 mL) were added. The volume was reduced on a rotary evaporator until a precipitate appeared, and then the solution was allowed to set at low temperature for 1 day to obtain a good precipitate. The solid was filtered on a frit, washed with cold water (3 × 5 mL) and ether (3 × 5 mL), and dried under vacuum. Yields and characterizations are given below.

*{[Ru^{II}$_2$(trpy)$_2$(μ-Cl)](μ-bpp-bz)}(PF$_6$)$_2$ [**4(PF$_6$)$_2$**]*. Yield: 199 mg (63%). Elem anal. Calcd for ($C_{50}H_{37}N_{10}Ru_2P_2F_{12}$): C, 46.0; H, 2.8; N, 10.7. Found: C, 45.9; H, 2.9; N, 10.6. ^{1}H NMR (400 MHz, acetone-d_6): δ 8.66 (d, 4 H, $^3J_{23-24}$ = 8.12 Hz, H23), 8.52 (ddd, 4 H, $^3J_{20-19}$ = 8.06 Hz, $^4J_{20-18}$ = 1.31 Hz, $^5J_{20-17}$ = 0.72 Hz, H20), 8.37 (ddd, 4 H, $^3J_{17-18}$ = 5.50 Hz, $^4J_{17-19}$ = 1.51 Hz, $^5J_{17-20}$ = 0.72 Hz, H17), 8.15 (t, 2 H, $^3J_{24-23}$ = 8.12 Hz, H24), 8.10 (ddd, 2 H, $^3J_{11-12}$ = 8.17 Hz, $^4J_{11-13}$ = 1.4 Hz, $^5J_{11-14}$ = 0.78 Hz, H11), 7.95 (ddd, 4 H, $^3J_{19-20}$ = 8.06 Hz, $^3J_{19-18}$ = 7.65 Hz, $^4J_{19-17}$ = 1.51 Hz, H19), 7.72 (ddd, 2 H, $^3J_{12-11}$ = 8.17 Hz, $^3J_{12-13}$ = 7.49 Hz, $^4J_{12-14}$ = 1.50 Hz, H12), 7.71 (d, 2 H, $^3J_{2-3}$ = 7.56 Hz, H2, H6), 7.60 (ddd, 4 H, $^3J_{18-19}$ = 7.65 Hz, $^3J_{18-17}$ = 5.50 Hz, $^4J_{18-10}$ = 1.31 Hz, H18), 7.47 (ddd, 2 H, $^3J_{14-13}$ = 5.65 Hz, $^4J_{14-12}$ = 1.50 Hz, $^5J_{14-11}$ = 0.78 Hz, H14), 7.45 (t, 2 H, $^3J_{3-2,4}$ = 7.56 Hz, 3H, 5H), 7.34 (t, 1 H, $^3J_{4-3,5}$ = 7.56 Hz, 4H), 6.77 (ddd, 2 H, $^3J_{13-12}$ = 7.49 Hz, $^3J_{13-14}$ = 5.65 Hz, $^4J_{13-11}$ = 1.40 Hz, H13), 5.24 (s, 2H, H14) . ^{13}C{^{1}H} NMR (100.6 MHz, acetone-d_6): δ 160.214 (C21), 159.787 (C10), 159.459 (C22), 154.792 (C14), 154.156 (C17), 147.480 (C9), 140.236 (C1), 138.036 (C19), 137.582 (C12), 134.912 (C24), 129.934 (C3), 129.115 (C2), 128.216 (C18), 127.565 (C4), 124.507 (C20), 123.344 (C23), 122.834 (C13), 121.284 (C11), 120.987 (C8), 30.78 (C7). ESI-MS (MeOH): *m*/*z* 1161 ([M − PF$_6^-$]$^+$). UV−vis (CH_2Cl_2) [λ_{max}, nm (ε, M^{-1} cm^{-1})]: 279 (59 516), 317 (56 452), 387 (25 226), 477 (16 581), 503 (15 032).

*{[Ru^{II}$_2$(trpy)$_2$(μ-Cl)]$_2$(μ-(bpp)$_2$-p-xyl)}(PF$_6$)$_4$ [**7(PF$_6$)$_4$**]*. Yield: 120 mg (44%). ^{1}H NMR (250 MHz, acetone-d_6): δ 8.66 (d, 8 H, $^3J_{23-24}$ = 8.09 Hz, H23), 8.52 (ddd, 8 H, $^3J_{20-19}$ = 8.38 Hz, $^4J_{20-18}$ = 1.25 Hz, $^5J_{20-17}$ = 0.6 Hz, H20), 8.35 (ddd, 8 H, $^3J_{17-18}$ = 5.53 Hz, $^4J_{17-19}$ = 1.33 Hz, $^5J_{17-20}$ = 0.6 Hz, H17), 8.15 (t, 4 H, $^3J_{24-23}$ = 8.09 Hz, H24), 8.07 (ddd, 4 H, $^3J_{14-13}$ = 8.08 Hz, $^4J_{14-12}$ = 1.30 Hz, $^5J_{14-11}$ = 0.63 Hz, H14), 7.93 (ddd, 8 H, $^3J_{19-20}$ = 8.38 Hz, $^3J_{19-18}$ = 7.38 Hz, $^4J_{19-17}$ = 1.37 Hz, H19), 7.87 (s, 4 H, H2, H3, H5, H6), 7.61 (ddd, 8 H, $^3J_{18-19}$ = 7.38 Hz, $^3J_{18-17}$ = 5.53 Hz, $^4J_{18-10}$ = 1.25 Hz, H18), 7.59 (ddd, 4 H, $^3J_{13-14}$ = 8.08 Hz, $^3J_{13-12}$ = 7.49 Hz, $^4J_{13-11}$ = 1.45 Hz, H13), 7.46 (ddd, 4 H, $^3J_{11-12}$ = 5.78 Hz, $^4J_{11-13}$ = 1.45 Hz, $^5J_{11-14}$ = 0.63 Hz, H11), 6.71 (ddd, 4 H$_{12}$, $^3J_{12-13}$ = 7.49 Hz, $^3J_{12-11}$ = 5.78 Hz, $^4J_{12-14}$ = 1.30 Hz, H12), 5.25 (s, 4 H, H7) . ^{13}C{^{1}H} NMR (62.9 MHz, acetone-d_6): δ 160.21 (C21), 159.78 (C11), 159.45 (C22), 154.77 (C11), 154.08 (C17), 147.47 (C9), 138.82 (C2, C5), 138.03 (C19), 137.47 (C13), 134.92 (C24), 129.92 (C2, C3, C5, C6), 128.22 (C18), 124.54 (C10), 123.36 (C23), 122.82 (C12), 121.36 (C14), 121.26 (C8), 30.59 (C7). UV−vis (CH_2Cl_2) [λ_{max}, nm (ε, M^{-1} cm^{-1})]: 276 (118 562), 315 (102 710), 383 (43 273), 476 (29 974), 507 (27 410). ESI-MS (MeOH): *m*/*z* 1121.5 ([M − 2PF$_6^-$]$^{2+}$).

*{[Ru^{II}$_2$(trpy)$_2$(μ-Cl)]$_2$(μ-(bpp)$_2$-m-xyl)}(PF$_6$)$_4$ [**8(PF$_6$)$_4$**]*. Yield: 92 mg (34%). ^{1}H NMR (400 MHz, acetone-d_6): δ 8.62 (d, 8 H, $^3J_{23-24}$ = 8.10 Hz, H23), 8.48 (d, 8 H, $^3J_{20-19}$ = 7.80 Hz, H20), 8.37 (dd, 8 H, $^3J_{17-18}$ = 5.46 Hz, $^4J_{17-19}$ = 1.10 Hz, H17), 8.23 (s, 1 H, H6), 8.10 (t, 4 H, $^3J_{24-23}$ = 8.10 Hz, H24), 8.04 (d, 4 H, $^3J_{11-12}$ = 7.52 Hz, H11), 7.89 (td, 8 H, $^3J_{19-18,20}$ = 7.8 Hz, $^4J_{19-17}$ = 1.10 Hz, H19), 7.64 (ddd, 8 H, $^3J_{18-19}$ = 7.80 Hz, $^3J_{18-17}$ = 5.46 Hz, $^4J_{18-20}$ = 0.80 Hz, H18), 7.64−7.54 (m, 3 H, H2, H3, H4), 7.46 (t, 4 H, $^3J_{12-13,11}$ = 7.52 Hz, H12), 7.45 (d, 4 H, $^3J_{14-13}$ = 6.21 Hz, H14), 6.69 (ddd, 4 H, $^3J_{13-12}$ = 7.52 Hz, $^3J_{13-14}$ = 6.21 Hz, $^4J_{13-11}$ = 1.35 Hz, H13), 5.38 (s, 4 H, H7) . ^{13}C{^{1}H} NMR (100.6 MHz, acetone-d_6): δ 160.16 (C21), 159.80 (C10), 159.42 (C22), 154.77 (C14), 154.10 (C17), 147.48 (C8), 141.19 (C1, C4), 138.01 (C19), 137.38 (C12), 134.90 (C24), 131.09 (C2, C4, or C3), 129.62 (C6), 128.33 (C18), 127.12 (C3 or C2, C4), 124.51 (C20), 123.33 (C23), 122.77 (C13), 121.20 (C11), 121.10 (C9). UV−vis (CH_2Cl_2) [λ_{max}, nm (ε, M^{-1} cm^{-1})]: 275 (121 704), 315 (99 987), 383 (41 593), 476 (29 333), 507 (26 646). ESI-MS (MeOH): *m*/*z* 2388.3 ([M − PF$_6^-$]$^+$).

*{[Ru^{II}$_2$(trpy)$_2$(μ-Cl)]$_2$(μ-(bpp)$_2$-o-xyl)}(PF$_6$)$_4$ [**9(PF$_6$)$_4$**]*. Yield: 111 mg (41%). ^{1}H NMR (360 MHz, acetone-d_6): δ 8.68 (d, 8 H, $^3J_{23-24}$ = 8.10 Hz, H23), 8.55 (d, 8 H, $^3J_{20-19}$ = 7.85 Hz, H20), 8.49 (dd, 8 H, $^3J_{17-18}$ = 5.42 Hz, $^4J_{17-19}$ = 1.40 Hz, H17), 8.16 (t, 4 H, $^3J_{24-23}$ = 8.10 Hz, H24), 7.99 (d, 4 H, $^3J_{11-12}$ = 7.65 Hz, H11), 7.97 (td, 8 H, $^3J_{19-18,20}$ = 7.85 Hz, $^4J_{19-17}$ = 1.40 Hz, H19), 7.84 (dd, 2 H, $^3J_{2-3}$ = 5.50 Hz, $^4J_{2-4}$ = 3.40 Hz, H2, H5), 7.67 (ddd, 8 H, $^3J_{18-19}$ = 7.85 Hz, $^3J_{18-17}$ = 5.42 Hz, $^4J_{18-20}$ = 1.20 Hz, H18), 7.62 (td, 4 H, $^3J_{12-13,11}$ = 7.65 Hz, $^4J_{12-14}$ = 1.35 Hz, H12), 7.51 (ddd, 4 H, $^3J_{14-13}$ = 5.65 Hz, $^4J_{14-12}$ = 1.35 Hz, $^5J_{14-11}$ = 0.50 Hz, H14), 7.38 (dd, 2 H, $^3J_{3-2}$ = 5.50 Hz, $^4J_{3-5}$ = 3.40 Hz, H3, H4), 6.75 (ddd, 4 H, $^3J_{13-12}$ = 7.65 Hz, $^3J_{13-14}$ = 5.65 Hz, $^4J_{13-11}$ = 1.30 Hz, H13), 5.76 (s, 4 H, H7). ^{13}C{^{1}H} NMR (90.5 MHz, acetone-d_6): δ 160.22 (C21), 159.92 (C10), 159.52 (C22), 154.84 (C14), 154.30 (C17), 147.97 (C8), 138.30 (C1, C6), 138.05 (C19), 137.37 (C12), 134.92 (C24), 128.57 (C2, C5), 128.52 (C3, C4), 128.35 (C18), 124.53 (C20), 123.35 (C23), 122.82 (C13), 121.38 (C11), 120.20 (C9), 28.72 (C7).

dx.doi.org/10.1021/ic101802y |*Inorg. Chem.* 2011, 50, 2771–2781

UV−vis (CH_2Cl_2) [λ_{max}, nm (ε, M^{-1} cm^{-1})]: 275 (116 467), 315 (97 546), 385 (41 279), 476 (30 420), 507 (27 092). ESI-MS (MeOH): m/z 2388.3 ([M − PF_6^-]$^+$).

General Synthetic Procedure for Complexes 5(PF$_6$)$_2$, 10(PF$_6$)$_4$, 11(PF$_6$)$_4$, and 12(PF$_6$)$_4$. A sample of 0.200 g (0.154 mmol of **4**(PF$_6$)$_2$ or 0.079 mmol of **7**(PF$_6$)$_4$, **8**(PF$_6$)$_4$ or **9**(PF$_6$)$_4$) of the chloro-bridged complex, 0.105 g (0.77 mmol) for **4**(PF$_6$)$_2$ or 0.240 g (1.76 mmol) for **7**(PF$_6$)$_4$, **8**(PF$_6$)$_4$, or **9**(PF$_6$)$_4$ of sodium acetate and a stoichiometric amount of $AgBF_4$ were dissolved in acetone/water (3:1, 40 mL) and heated at reflux temperature overnight. The resulting solution was filtered, and a saturated aqueous NH_4PF_6 solution (1 mL) was added. Upon reduction of the volume, a solid precipitated from the solution and was washed with cold water and ether. Yields and characterizations are given below.

{[Ru^{II}_2(trpy)$_2$(μ-OAc)](μ-bpp-bz)}(PF$_6$)$_2$ [**5(PF$_6$)$_2$**]. Yield: 174 mg (86%). Elem anal. Calcd for ($C_{52}H_{40}N_{10}Ru_2O_2P_2F_{12}$): C, 47.0; H, 3.0; N, 10.5. Found: C, 47.1; H, 3.3; N, 10.1. ^{1}H NMR (250 MHz, acetone-d_6): δ 8.72 (d, 4 H, $^3J_{23-24}$ = 8.04 Hz, H23), 8.61 (ddd, 4 H, $^3J_{20-19}$ = 7.90 Hz, $^4J_{20-18}$ = 1.24 Hz, $^5J_{20-17}$ = 0.68 Hz, H20), 8.41 (ddd, 4 H, $^3J_{17-18}$ = 5.50 Hz, $^4J_{17-19}$ = 1.49 Hz, $^5J_{17-20}$ = 0.68 Hz, H17), 8.19 (t, 2 H, $^3J_{24-23}$ = 8.04 Hz, H24), 8.04 (ddd, 2 H, $^3J_{11-12}$ = 8.15 Hz, $^4J_{11-13}$ = 1.35 Hz, $^5J_{11-14}$ = 0.80 Hz, H11), 8.02 (td, 4 H, $^3J_{19-20,18}$ = 7.90 Hz, $^4J_{19-17}$ = 1.49 Hz, H19), 7.63 (d, 2 H, $^3J_{2-3}$ = 7.25 Hz, H2, H6), 7.62 (ddd, 2 H, $^3J_{12-11}$ = 8.15 Hz, $^3J_{12-13}$ = 7.40 Hz, $^4J_{12-14}$ = 1.47 Hz, H12), 7.48 (ddd, 4H, $^3J_{18-19}$ = 7.90 Hz, $^3J_{18-17}$ = 5.50 Hz, $^4J_{18-20}$ = 1.24 Hz, H18), 7.42 (ddd, 2H, $^3J_{14-13}$ = 5.80 Hz, $^4J_{14-12}$ = 1.47 Hz, $^5J_{14-11}$ = 0.80 Hz, H14), 7.40 (t, 2 H, $^3J_{3-2,1}$ = 7.25 Hz, H3, H5), 7.28 (t, 1 H, $^3J_{4-3,5}$ = 7.56 Hz, H4), 6.79 (ddd, 2 H, $^3J_{13-12}$ = 7.40 Hz, $^3J_{13-14}$ = 5.80 Hz, $^4J_{13-11}$ = 1.35 Hz, H13), 5.17 (s, 2 H, H14), 0.41 (s, 3 H, CH_3 acetate). ^{13}C{^{1}H} NMR (62.9 MHz, acetone-d_6): δ 159.72 (C21), 159.62 (C22), 156.55 (C10), 153.74 (C17), 153.00 (C14), 149.84 (C9), 138.50 (C1), 137.27 (C19), 135.64 (C12), 133.87 (C24), 128.86 (C3, C5), 128.13 (C2, C6), 127.25 (C18), 126.58 (C4), 123.52 (C20), 122.61 (C23), 121.86 (C13), 119.75 (C8), 119.57 (C11), 29.72 (C7), 29.07 (CH_3 acetate). UV−vis (CH_2Cl_2) [λ_{max}, nm (ε, M^{-1} cm^{-1})]: 277 (74 000), 317 (68 000), 379 (31 000), 499 (16 133), 537 (13 600). ESI-MS (MeOH): m/z 1185 ([M − PF_6^-]$^+$).

{[Ru^{II}_2(trpy)$_2$(μ-OAc)]$_2$(μ-(bpp)$_2$-p-xyl)}(PF$_6$)$_4$ [**10(PF$_6$)$_4$**]. Yield: 85 mg (84%). ^{1}H NMR (250 MHz, acetone-d_6): δ 8.71 (d, 8 H, $^3J_{23-24}$ = 8.12 Hz, H23), 8.58 (ddd, 8 H, $^3J_{20-19}$ = 8.39 Hz, $^4J_{20-18}$ = 1.19 Hz, $^5J_{20-17}$ = 0.65 Hz, H20), 8.32 (ddd, 8 H, $^3J_{17-18}$ = 5.54 Hz, $^4J_{17-19}$ = 1.48 Hz, $^5J_{17-10}$ = 0.65 Hz, H17), 8.18 (t, 4 H, $^3J_{24-23}$ = 8.12 Hz, H24), 8.03 (ddd, 4 H, $^3J_{14-13}$ = 8.16 Hz, $^4J_{14-12}$ = 1.32 Hz, $^5J_{14-11}$ = 0.67 Hz, H14), 7.95 (ddd, 8 H, $^3J_{19-20}$ = 8.39 Hz, $^3J_{19-18}$ = 7.38 Hz, $^4J_{19-17}$ = 1.48 Hz, H19), 7.69 (s, 4 H, H2, H3, H5, H6), 7.53 (ddd, 4 H, $^3J_{13-14}$ = 8.16 Hz, $^3J_{13-12}$ = 7.52 Hz, $^4J_{13-11}$ = 1.42 Hz, H13), 7.42 (ddd, 4 H, $^3J_{11-12}$ = 5.88 Hz, $^4J_{11-13}$ = 1.42 Hz, $^5J_{11-14}$ = 0.67 Hz, H11), 7.39 (ddd, 8 H, $^3J_{18-19}$ = 7.38 Hz, $^3J_{18-17}$ = 5.54 Hz, $^4J_{18-10}$ = 1.19 Hz, H18), 6.78 (ddd, 4 H, $^3J_{12-13}$ = 7.52 Hz, $^3J_{12-11}$ = 5.88 Hz, $^4J_{12-14}$ = 1.32 Hz, H12), 5.13 (s, 4 H, H7), 0.39 (s, 6 H, CH_3 acetate). ^{13}C{^{1}H} NMR (62.9 MHz, acetone-d_6): δ 192.95 (CO acetate), 160.64 (C22), 160.61 (C21), 157.55 (C10), 154.60 (C17), 154.03 (C14), 150.77 (C8), 138.25 (C19), 136.56 (C13), 134.93 (C24), 129.85 (C1, C2, C3, C4, C5, C6), 128.16 (C18), 126.55 (C11), 124.55 (C20), 123.65 (C23), 122.92 (C12), 121.03 (C9) 120.59 (C11), 26.05 (CH_3 acetate). UV−vis (CH_2Cl_2) [λ_{max}, nm (ε, M^{-1} cm^{-1})]: 276 (130 250), 317 (110 625), 375 (46 525), 496 (26 575), 532 (23 356). ESI-MS (MeOH): m/z 1145 ([M − 2PF_6^-]$^{2+}$).

{[Ru^{II}_2(trpy)$_2$(μ-OAc)]$_2$(μ-(bpp)$_2$-m-xyl)}(PF$_6$)$_4$ [**11(PF$_6$)$_4$**]. Yield: 88 mg (86%). ^{1}H NMR (400 MHz, acetone-d_6): δ 8.71 (d, 8 H, $^3J_{23-24}$ = 8.09 Hz, H23), 8.59 (ddd, 8 H, $^3J_{20-19}$ = 7.90 Hz, $^4J_{20-18}$ = 1.35 Hz, $^5J_{20-17}$ = 0.75 Hz, H20), 8.41 (ddd, 8 H, $^3J_{17-18}$ = 5.60 Hz, $^4J_{17-19}$ = 1.60 Hz, $^5J_{17-20}$ = 0.75 Hz, H17), 8.19 (t, 4 H, $^3J_{24-23}$ = 8.09 Hz, H24), 8.15 (s, 1 H, H6), 7.99 (dd, 4 H, $^3J_{11-12}$ = 7.98 Hz, $^4J_{11-7}$ = 1.28 Hz, H11), 7.98 (td, 8 H, $^3J_{19-18,20}$ = 7.90 Hz, $^4J_{19-17}$ = 1.60 Hz, H19), 7.49 (ddd, 8 H, $^3J_{18-19}$ = 7.90 Hz, $^3J_{18-17}$ = 5.60 Hz, $^4J_{18-20}$ = 1.35 Hz, H18), 7.46−7.38 (m, 11 H, H14, H12, H2, H3, H4), 6.74 (ddd, 4 H, $^3J_{13-12}$ = 7.56 Hz, $^3J_{13-14}$ = 5.79 Hz, $^4J_{13-11}$ = 1.28 Hz, H13), 5.26 (s, 4 H, H7), 0.42 (s, 6 H, CH_3 acetate). ^{13}C{^{1}H} NMR (100.6 MHz, acetone-d_6): δ 192.85 (CO acetate), 160.71 (C22), 160.59 (C21), 157.55 (C10), 154.69 (C17), 154.03 (C14), 150.87 (C8), 140.44 (C1, C5), 138.26 (C19), 136.44 (C12), 134.90 (C24), 130.77 (C3), 129.98 (C6), 128.31 (C18), 127.03 (C2, C4), 124.53 (C20), 123.60 (C23), 122.83 (C13), 120.69 (C9), 120.49 (C11), 30.92 (C7), 26.07 (CH_3 acetate). UV−vis (CH_2Cl_2) [λ_{max}, nm (ε, M^{-1} cm^{-1})]: 276 (131 026), 317 (119 448), 375 (52 950), 496 (29 938), 532 (25 825). ESI-MS (MeOH): m/z 2436.3 ([M − PF_6]$^+$).

{[Ru^{II}_2(trpy)$_2$(μ-OAc)]$_2$(μ-(bpp)$_2$-o-xyl)}(PF$_6$)$_4$ [**12(PF$_6$)$_4$**]. Yield: 61 mg (60%). ^{1}H NMR (400 MHz, acetone-d_6): δ 8.73 (d, 8 H, $^3J_{23-24}$ = 8.10 Hz, H23), 8.62 (d, 8 H, $^3J_{20-19}$ = 7.95 Hz, H20), 8.52 (d, 8H, $^3J_{17-18}$ = 5.30 Hz, H17), 8.20 (t, 4 H, $^3J_{24-23}$ = 8.10 Hz, H24), 8.03 (td, 8 H, $^3J_{19-18,20}$ = 7.95 Hz, $^4J_{19-17}$ = 1.20 Hz, H19), 7.96 (ddd, 4 H, $^3J_{11-12}$ = 8.00 Hz, $^4J_{11-13}$ = 1.30 Hz, $^5J_{11-14}$ = 0.65 Hz, H11), 7.68 (dd, 2 H, $^3J_{2-3}$ = 5.40 Hz, $^4J_{2-4}$ = 3.40 Hz, H2, H5), 7.59 (td, 4 H, $^3J_{12-11,13}$ = 8.00 Hz, $^4J_{12-14}$ = 1.40 Hz, H12), 7.53 (ddd, 8 H, $^3J_{18-19}$ = 7.95 Hz, $^3J_{18-17}$ = 5.30 Hz, $^4J_{18-10}$ = 1.20 Hz, H18), 7.46 (ddd, 4 H, $^3J_{14-13}$ = 5.75 Hz, $^4J_{14-12}$ = 1.40 Hz, $^5J_{14-11}$ = 0.65 Hz, H14), 7.28 (dd, 2 H, $^3J_{3-2}$ = 5.40 Hz, $^4J_{3-5}$ = 3.40 Hz, H3, H4), 6.78 (ddd, 4 H, $^3J_{13-12}$ = 8.00 Hz, $^3J_{13-14}$ = 5.75 Hz, $^4J_{13-11}$ = 1.30 Hz, H13), 5.62 (s, 4 H, H7), 0.44 (s, 6 H, CH_3 acetate). ^{13}C{^{1}H} NMR (100.6 MHz, acetone-d_6): δ 193.00 (CO acetate), 160.70 (C22), 160.62 (C21), 157.53 (C10), 154.75 (C17), 154.08 (C14), 151.24 (C8), 138.33 (C19), 137.49 (C1, C6), 136.59 (C12), 134.95 (C24), 128.53 (C2, C3, C4, C5), 128.30 (C18), 124.56 (C20), 123.63 (C23), 122.89 (C13), 120.52 (C11), 119.65 (C9), 30.59 (C7), 26.09 (CH_3 acetate). UV−vis (CH_2Cl_2) [λ_{max}, nm (ε, M^{-1} cm^{-1})]: 276 (127 725), 317 (118 418), 376 (51 380), 496 (30 546), 532 (25 992). ESI-MS (MeOH): m/z 2436.3 ([M − PF_6]$^+$).

General Synthetic Procedure for Complexes 6^{3+}, 13^{6+}, 14^{6+}, and 15^{6+}. These complexes can be prepared by hydrolysis of the acetate-bridged precursor complexes (**5**(PF$_6$)$_2$, **10**(PF$_6$)$_4$, **11**(PF$_6$)$_4$, and **12**(PF$_6$)$_4$) in acidic aqueous media. Even though the NMR experiments obtained by dissolving the acetate-bridged complexes in acidic media show the presence of pure aqua complexes, we could not isolate a solid material, presumably because of replacement of the aqua ligands by the anions present in the solution.

{[Ru^{II}_2(trpy)$_2$(H_2O)$_2$](μ-bpp-bz)}$^{3+}$ [**6^{3+}**]. ^{1}H NMR (400 MHz, acetone-d_6/D_2O/a drop of CF_3COOD): δ 8.49 (d, 4 H, $^3J_{23-24}$ = 8.00 Hz, H23), 8.37 (d, 4H, $^3J_{20-19}$ = 7.94 Hz, H20), 8.18 (d, 4 H, $^3J_{17-18}$ = 4.30 Hz, H17), 8.07 (t, 2 H, $^3J_{24-23}$ = 8.00 Hz, H24), 7.87 (td, 4 H, $^3J_{19-20,18}$ = 7.94 Hz, H19), 7.86 (d, 2 H, $^3J_{11-12}$ = 7.94 Hz, H11), 7.46 (t, 2 H, $^3J_{12-11}$ = 7.94 Hz, H12), 7.45 (d, 2 H, $^3J_{2-3}$ = 7.45 Hz, H2, H6), 7.35−7.24 (m, 8 H, H18, H14, H3, H5), 7.16 (t, 1 H, $^3J_{4-3,5}$ = 7.46 Hz, H4), 6.63 (t, 2 H, $^3J_{13-14}$ = 5.80 Hz, H12), 5.01 (s, 2 H, H7). ^{13}C{^{1}H} NMR (100.6 MHz, acetone-d_6/D_2O/a drop of CF_3COOD): δ 154.15 (C17), 153.84 (C14), 138.66 (C19), 136.49 (C12), 136.09 (C24), 129.65 (C18), 128.03 (C4), 127.47 (C3, C5), 124.44 (C20), 123.39 (C23), 122.74 (C13).

{[Ru^{II}_2(trpy)$_2$(H_2O)$_2$]$_2$(μ-(bpp)$_2$-p-xyl)}$^{6+}$ [**13^{6+}**]. ^{1}H NMR (400 MHz, acetone-d_6/D_2O/a drop of triflic acid): δ 8.60 (d, 8 H, $^3J_{23-24}$ = 8.20 Hz, H23), 8.47 (d, 8 H, $^3J_{20-19}$ = 7.90 Hz, H20), 8.14 (t, 4 H, $^3J_{24-23}$ = 8.20 Hz, H24), 8.10 (d, 8 H, $^3J_{17-18}$ = 5.50 Hz, H17), 7.86 (d, 4 H, $^3J_{11-12}$ = 8.00 Hz, H11), 7.84 (t, 8 H, $^3J_{19-20,18}$ = 7.90 Hz, H19), 7.47 (s, 4 H, H2, H3, H5, H6), 7.44 (dd, 4 H, $^3J_{12-11}$ = 8.00 Hz, $^3J_{12-13}$ = 7.50 Hz, H12), 7.29 (dd, 8 H, $^3J_{18-19}$ = 7.90 Hz, $^3J_{18-17}$ = 5.50 Hz, H18), 7.25 (d, 4 H, $^3J_{14-13}$ = 5.70 Hz, H14), 6.76 (dd, 4 H, $^3J_{13-12}$ = 7.50 Hz, $^3J_{13-14}$ = 5.70 Hz, H13). ^{13}C{^{1}H} NMR (100.6 MHz, acetone-d_6/D_2O/a drop of triflic acid): δ 154.43 (C17), 152.14 (C14), 138.67 (C19), 136.34 (C24, C12), 129.42 (C2, C3, C5, C6), 128.59 (C18), 124.62 (C20), 123.90 (C23), 123.20 (C13), 120.68 (C11).

{[Ru^{II}_2(trpy)$_2$(H_2O)$_2$]$_2$(μ-(bpp)$_2$-m-xyl)}$^{6+}$ [**14^{6+}**]. ^{1}H NMR (400 MHz, acetone-d_6/D_2O/a drop of CF_3COOD): δ 8.47 (d, 8 H, $^3J_{23-24}$ = 8.45 Hz,

dx.doi.org/10.1021/ic101802y |Inorg. Chem. 2011, 50, 2771–2781

Table 1. Crystallographic Data for Complexes 4^{2+}, 5^{2+}, and 11^{4+}

	$4(PF_6)_2 \cdot 1C_3H_6O \cdot 0.32H_2O$	$5(PF_6)_2$	$11(PF_6)_4 \cdot 4.5C_2H_6O \cdot 2.5H_2O$
empirical formula	$C_{54}H_{47.65}ClF_{12}N_{10}O_{1..32}P_2Ru_2$	$C_{52}H_{40}F_{12}N_{10}O_2P_2Ru_2$	$C_{55.25}H_{50.50}F_{12}N_{10}O_5P_2Ru_2$
fw	1385.36	1329.02	1426.64
temperature, K	100(2)	100(2)	100(2)
wavelength, Å	0.710 73	0.710 73	0.710 73
cryst syst	triclinic	triclinic	orthorhombic
space group	$P\bar{1}$	$P\bar{1}$	$Pmn2(1)$
a, Å	14.6370(8)	12.6872(7)	25.3428(10)
α, deg	98.898(2)	90.713(3)	90.00
b, Å	19.5535(10)	14.1522(10)	17.2007(7)
β, deg	103.603(2)	111.643(3)	90.00
c, Å	20.3342(11)	17.0548(10)	14.7026(6)
γ, deg	102.698(3)	91.573(3)	90.00
V, Å^3	5385.8(5)	2844.4(3)	6409.0(4)
Z	4	2	4
ρ, g/cm^3	1.709	1.552	1.479
R $[I > 2\sigma(I)]^a$	0.0385	0.0717	0.0883
wR	0.0969	0.1677	0.2392

^{a} $R = \Sigma[F_o - F_c]/\Sigma F_o$; $wR = \{\Sigma[w(F_o^2 - F_c^2)^2]/\Sigma(wF_o^4)\}^{1/2}$.

H23), 8.35 (d, 8 H, $^3J_{20-19}$ = 8.00 Hz, H20), 8.19 (d, 8 H, $^3J_{17-18}$ = 4.32 Hz, H17), 8.07 (t, 4 H, $^3J_{24-23}$ = 8.45 Hz, H23), 7.93 (s, 1 H, H6), 7.86−7.77 (m, 4 H, H11), 7.82 (t, 8 H, $^3J_{19-20,18}$ = 8.00 Hz), 7.36−7.24 (m, 15 H, H18, H14, H2, H3, H4), 7.21 (t, 4 H, $^3J_{12-13,11}$ = 6.50 Hz, H12), 6.58 (t, 4 H, $^3J_{13-12}$ = 6.5 Hz, H13), 5.10 (s, 4 H, H7). $^{13}C\{^1H\}$ NMR (100.6 MHz, acetone-d_6/D_2O/a drop of CF_3COOD): δ 154.04 (C17), 153.86 (C14), 138.60 (C19), 136.12 (C24), 135.47 (C12), 127.92 (C18), 124.43 (C20), 123.38 (C19), 122.59 (C13).

{[Ru^{II}$_2$(trpy)$_2$(H$_2$O)$_2$]$_2$(μ-(bpp)$_2$-o-xyl)}$^{6+}$ [**15**$^{6+}$]. ^{1}H NMR (400 MHz, acetone-d_6/D_2O/a drop of CF_3COOD): δ 8.39 (d, 8 H, $^3J_{23-24}$ = 8.04 Hz, H23), 8.28 (d, 8 H, $^3J_{20-19}$ = 8.04 Hz, H20), 8.23 (d, 8 H, $^3J_{17-18}$= 4.70 Hz, H17), 8.03 (t, 4 H, $^3J_{24-23}$ = 8.04 Hz, H24), 7.82 (t, 8 H, $^3J_{19-18,20}$ = 8.04 Hz, H19), 7.76 (d, 4 H, $^3J_{11-12}$ = 8.00 Hz, H11), 7.48 (dd, 2 H, $^3J_{2-3}$ = 5.40 Hz, $^4J_{2-4}$ = 3.40 Hz, H2, H5), 7.37 (t, 4 H, $^3J_{12-11,13}$ = 8.00 Hz, H12), 7.32−7.23 (m, 12 H, H18, H14), 7.19 (dd, 2 H, $^3J_{3-2}$ = 5.40 Hz, $^4J_{3-5}$ = 3.40 Hz, H3), 5.39 (s, 4 H, H7). $^{13}C\{^1H\}$ NMR (100.6 Mz, acetone-d_6/D_2O/a drop of CF_3COOD): δ 154.27 (C17), 154.00 (C14), 150.89 (C8), 138.53 (C19), 136.23 (C12), 136.19 (C24), 128.55−128.14 (C2, C3, C4, C5, C18), 124.36 (C20), 123.42 (C23).

Instrumentation and Measurements. UV−vis spectroscopy was performed by a HP8453 spectrometer using 1 cm quartz cells. ^{1}H NMR spectroscopy was performed on a Bruker DPX 250 MHz, a Bruker DPX 360 MHz, or a Bruker DPX 400 MHz spectrometer. Samples were run in $CDCl_3$, acetone-d_6, or D_2O with internal references (residual protons and/or tetramethylsilane or DSS, respectively). Elemental analyses were performed using a Carlo Erba CHMS EA-1108 instrument provided by the Chemical Analysis Service of the Universitat Autonoma de Barcelona (CAS-UAB). Electrospray ionization mass spectrometry (ESI-MS) experiments were performed on a HP298s gas chromatography (GC)−MS system from the CAS-UAB. Cyclic voltammetry (CV) experiments were performed with a PAR283 potentiostat using a three-electrode cell. A glassy carbon disk (3 mm diameter) was used as the working electrode, platinum wire was used as the auxiliary electrode, and a saturated sodium calomel electrode (SSCE) was used as the reference electrode. For solutions of the complexes in organic solvents, n-Bu_4NPF_6 was used as the supporting electrolyte to yield a solution with 0.1 M ionic strength. In aqueous solutions, the CV experiments were carried out in the indicated pH buffer. All $E_{1/2}$ values reported here were estimated from CV as an average of the oxidative and reductive peak potentials ($E_{p,a} + E_{p,c}$)/2 and are referred to the SSCE reference electrode. For construction of the Pourbaix diagram, the following buffers were used: hydrogen phthalate/triflic acid up to pH = 4, hydrogen phthalate/sodium hydroxide for pH = 5, dihydrogen phosphate/sodium hydroxide for pH = 6, borax/triflic acid for pH = 7, and hydrogen phosphate/sodium hydroxide for the pH range 8−9. Also 0.1 M triflic acid was used for pH = 1.0. The concentration of the species was approximately 1 mM. Online manometric measurements were carried out on a Testo 521 differential pressure manometer with an operating range of 1−100 hPa and an accuracy within 0.5% of the measurement, coupled to thermostatted reaction vessels for dynamic monitoring of the headspace pressure above each reaction. The secondary ports of the manometers were connected to thermostatically controlled reaction vessels that contained the same solvents and headspace volumes as the sample vials. Online monitoring of the gas evolution was performed on a Pfeiffer Ominstar GSD 301C mass spectrometer. Typically, 16.04 mL degassed vials containing a suspension of the catalysts in 0.1 M triflic acid (1.5 mL) were connected to the apparatus capillary tubing. Subsequently, the previously degassed solution of cerium(IV) (0.5 mL) at pH = 1 (triflic acid, 200 equiv) was introduced using a Hamilton gastight syringe, and the reaction was dynamically monitored. A response ratio of 1:2 was observed when equal concentrations of dioxygen (O_2) and carbon dioxide (CO_2), respectively, were injected and thus was used for calculation of their relative concentrations.

X-ray Crystal Structure Determination. Crystals of 4^{2+}, 5^{2+}, and 11^{4+} were obtained by the slow diffusion of diethyl ether into an acetone solution containing the complexes **4**$(PF_6)_2$, **5**$(PF_6)_2$, and **11**$(PF_6)_4$ at room temperature. The **4**$(PF_6)_2$ crystals were grown as metallic plates, the **5**$(PF_6)_2$ ones as translucent plates, and the **11**$(PF_6)_4$ ones as brown plates. The measured crystals were prepared under inert conditions, immersed in perfluoropolyether as a protecting oil for manipulation.

Data collection was made on a Bruker-Nonius diffractometer equipped with an APEX II 4K CCD area detector, a FR591 rotating anode with Mo Kα radiation, Montel mirrors as a monochromator, and a Kryoflex low-temperature device (T = −173 °C). Full-sphere data collection was used with ω and φ scans. *Programs used:* data collection, *APEX II*,[18] data reduction, Bruker *Saint V/.60A*;[19] absorption correction, *SADABS*.[20]

Structure Solution and Refinement. For this, *SHELXTL*[21] was used. The crystal data parameters are listed in Table 1. For the structure of {[Ru^{II}$_2$(trpy)$_2$(μ-OAc)](μ-bpp-bz)}$(PF_6)_2$ [**5**$(PF_6)_2$], the program *SQUEEZE*[22] implemented in *PLATON*[23] was used to avoid highly disordered methanol molecules. In the structure {[Ru^{II}$_2$(trpy)$_2$(μ-OAc)]$_2$(μ-(bpp)$_2$-*m*-xyl)}$(PF_6)_4$ [**11**$(PF_6)_4$], the asymmetric unit is made up of half of a ruthenium complex with the acetate disordered over two positions with an

dx.doi.org/10.1021/ic101802y |*Inorg. Chem.* 2011, 50, 2771–2781

Scheme 2. Synthetic Strategy for the Complexes Described in This Work

L	x			
Hbpp	1	$\mathbf{1}^{2+}$	$\mathbf{2}^{2+}$	$\mathbf{3}^{3+}$
Hbpp-bz	1	$\mathbf{4}^{2+}$	$\mathbf{5}^{2+}$	$\mathbf{6}^{3+}$
$(Hbpp)_2$-*p*-xyl	2	$\mathbf{7}^{4+}$	$\mathbf{10}^{4+}$	$\mathbf{13}^{6+}$
$(Hbpp)_2$-*m*-xyl	2	$\mathbf{8}^{4+}$	$\mathbf{11}^{4+}$	$\mathbf{14}^{6+}$
$(Hbpp)_2$-*o*-xyl	2	$\mathbf{9}^{4+}$	$\mathbf{12}^{4+}$	$\mathbf{15}^{6+}$

occupation ratio of 90:10, two PF_6^- anions (one of them located over a mirror plane in the halves and each one with disorder), 2.25 acetone molecules over five positions (four of them with 0.5 occupancy and one with 0.25 occupancy), and 1.25 water molecules over five positions (one with 0.25 occupancy and four with 0.125 occupancy).

RESULTS AND DISCUSSION

Synthesis and Structure. The synthetic strategy to prepare the new Hbpp modified ligands is depicted in Scheme 1 and involves the nucleophilic addition of a halo derivative to the C atom of the β-diketone precursor or the nucleophilic substitution of the enolate, followed by reaction with hydrazine to generate the heterocyclic pyrazolate ring in good yield. For the Hbpp-bz ligand, the halo derivative used was benzyl bromide, whereas for the tetranucleating ligands $(Hbpp)_2$-*u*-xyl (*u* = *p*, *m*, or *o*), it was the corresponding *p*-, *m*-, or *o*-1,4-bis(halomethyl)benzene (halo = chloro or bromo). All of the new ligands were characterized by elemental analysis and the usual spectroscopic techniques. For the preparation of ruthenium complexes, we used $[RuCl_3(trpy)]$ as the metal precursor in combination with the free ligands just described (see Scheme 2). Under excess acetate and the presence of stoichiometric Ag^+, the Cl-bridging ligand can be easily replaced by the acetato-bridging ligand. The latter is then replaced by aqua ligands under acidic conditions. The formation of the aqua complex is further corroborated in the NMR spectra by the resonance shift of the methyl group of the acetato ligand from coordinated, 0.45 ppm, to free acetate, 1.95 ppm (see Figure S17 in the Supporting Information). All of the ruthenium complexes prepared in the present work were characterized by elemental analysis and spectroscopic techniques (UV−vis, MS, and NMR) together with their redox properties. The numbering scheme is presented in Scheme 2.

X-ray diffraction analysis was also carried out for complexes $\mathbf{4}^{2+}$, $\mathbf{5}^{2+}$, and $\mathbf{11}^{4+}$. Their crystallographic parameters are reported in Table 1, and views of their structures are presented in Figure 1. In all three complexes, the ruthenium metal centers adopt a pseudooctahedral coordination geometry with three positions occupied by the meridional trpy ligand, two by the tetradentate Hbpp-related ligand, and the final position either by a Cl-bridging ligand or by an O atom of the acetato-bridging ligand. In all cases, bond distances and angles are unremarkable, and thus similar to previous complexes already described in the literature.[24] An interesting feature that can be observed in the dinuclear complexes $\mathbf{4}^{2+}$ and $\mathbf{5}^{2+}$ is the different relative spatial dispositions of the trpy ligands. Whereas in the Cl-bridged complex they are situated orthogonally facing one another, in the acetato-bridged complex they are situated above and below the equatorial plane defined by the ruthenium metals and the two N atoms of the pyrazolate group. This is a consequence of the geometrical and steric demands imposed by the acetato ligand and the rigidity of the bpp^- framework. The same distortion is also

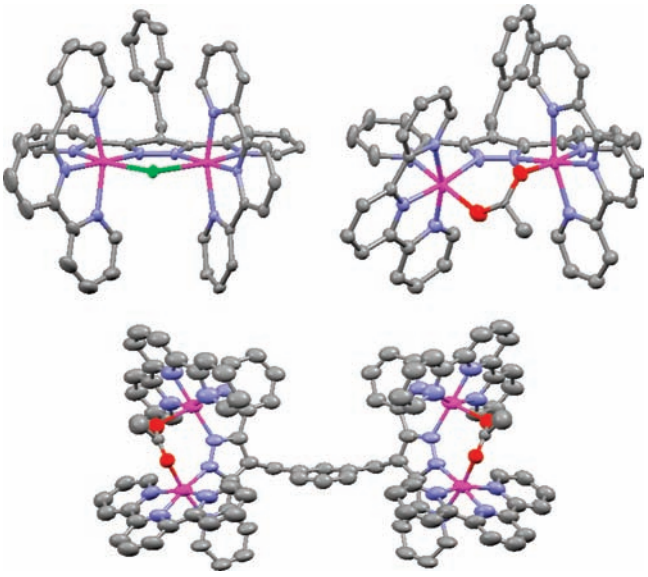

Figure 1. Mercury ellipsoid plot (50% probability) for the cationic part of complexes $\mathbf{4}^{2+}$ (top left), $\mathbf{5}^{2+}$ (top right), and $\mathbf{11}^{4+}$ (bottom). Color code: Ru, pink; Cl, green; N, blue; O, red. H atoms are not shown.

observed in the tetranuclear complex $\mathbf{11}^{4+}$, where the two dinuclear subunits are linked by the *m*-xylyl entity.

1D and 2D NMR spectroscopy allows structural characterization of all complexes in solution (see Figure 2, the Experimental Section, and the Supporting Information). All of the resonances observed in NMR spectra can be unambiguously assigned based on their integrals, symmetry, and multiplicity. The chloro-bridged dinuclear complex $\mathbf{4}^{2+}$ in solution displays C_{2v} geometry with one plane of symmetry containing the bpp part of the bpp-bz ligand as well as the two Ru centers, the Cl-bridging ligand, and the central N atom of the trpy moyeties. This plane bisects the trpy ligands and is perpendicular to a second symmetry plane that bisects the bpp-bz ligands and interconverts the two trpy ligands. The acetato-bridged complexes $\mathbf{5}^{2+}$ and $\mathbf{6}^{3+}$ have C_2 symmetry because, in order to accommodate the acetato-bridging ligand, the pseudooctahedral geometry of the Ru center has to be further distorted. As mentioned above, this results in one Ru center moving above the equatorial plane together with its trpy ligand, whereas the other metal center does the opposite. In solution at room temperature, these two complexes present dynamic behavior, with the two Ru centers synchronically moving very fast below and above the equatorial plane, and as a result, in the NMR the resonances can be assigned as if the complexes had C_{2v} symmetry. As a consequence of this, the external pyridyls of the trpy ligand appear as magnetically symmetric at room temperature.[25,11] For the tetranuclear complexes

dx.doi.org/10.1021/ic101802y |*Inorg. Chem.* 2011, 50, 2771–2781

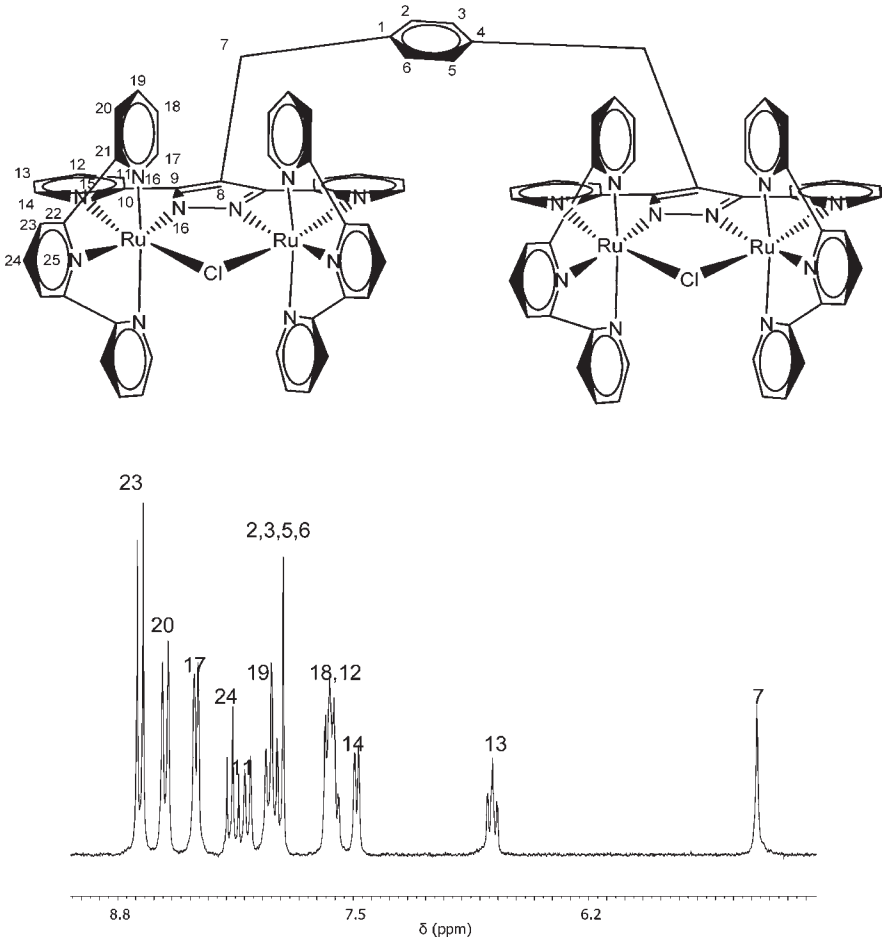

Figure 2. Drawn structure with atom labeling scheme and ^{1}H NMR (acetone-d_6) for $\mathbf{7}^{4+}$.

$\mathbf{7}^{4+}-\mathbf{12}^{4+}$ and $\mathbf{13}^{6+}-\mathbf{15}^{6+}$, their behavior is very similar to that of the dinuclear complexes just described, except for the resonances of the bridging xylyl linker. In other words, the two dinuclear sites of the tetranuclear complexes are undistinguishable in the NMR. This is a consequence of the presence of a C_2 axis that runs through the aromatic linker and interconverts each dinucleating unit and of the presence of a local C_2 (or pseudo C_2 in the case of the acetate and aquo complexes) that interconverts each trpy ligands of each dinuclear site. Figure 2 displays a drawn structure of complex $\mathbf{7}^{4+}$ including the atom labeling scheme for the ^{1}H NMR assignment together with its spectrum.

Spectroscopic and Redox Properties. The UV−vis spectral features in dichloromethane for the complexes described in this work are listed in the Experimental Section, and the UV−vis spectra for the chloro $\mathbf{7}^{4+}$, the acetate $\mathbf{10}^{4+}$, and the aqua $\mathbf{13}^{6+}$ are displayed in Figure 3 and are representative of the rest of the complexes. Three main regions can be distinguished: one between 200 and 350 nm, in which very intense bands are observed due to intraligand $\pi-\pi^*$ transitions; another one between 350 and 550 nm, in which there are mainly broad unsymmetrical Ru(dπ)−trpy/bpp(π^*) metal-to-ligand charge-transfer bands; and finally the region above 550 nm, in which d−d transitions are observed.[26]

Electrochemical experiments were carried out by means of CV and are presented in Figure 4. For the Cl^- and AcO^- complexes that do not contain aqua groups, the voltammograms in organic solvents show two chemically reversible and electrochemically quasi-reversible redox waves. Figure 4, left, shows the CV of complex $\mathbf{10}^{4+}$ in CH_2Cl_2

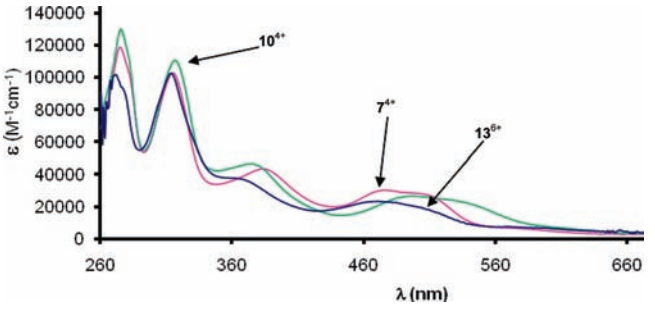

Figure 3. UV−vis spectra of 8 μM samples of complexes $\mathbf{7}^{4+}$ (pink) and $\mathbf{10}^{4+}$ (green) in CH_2Cl_2 and of 5 μM $\mathbf{13}^{6+}$ (blue) at pH = 1.0 in a 0.1 M triflic acid solution.

displaying two faradaic redox processes. The first redox process at 0.76 V is assigned to the formation of the mixed-valence species for each subunit (III−II + e^- → II−II) that occurs at exactly the same potential and thus manifests the independent behavior of each dimeric subunit.

$$\{[Ru^{III}Ru^{II}(trpy)_2(\mu\text{-}Cl)]_2(\mu\text{-}(bpp)_2\text{-}p\text{-}xyl)\}^{6+} + 2e^- \rightarrow \{[Ru^{II}Ru^{II}(trpy)_2(\mu\text{-}Cl)]_2(\mu\text{-}(bpp)_2\text{-}p\text{-}xyl)\}^{4+} \quad (2)$$

A second redox process is observed at 1.07 V and involves the removal of a second electron associated with III−III + e^- → III−II,

dx.doi.org/10.1021/ic101802y |*Inorg. Chem.* 2011, 50, 2771–2781

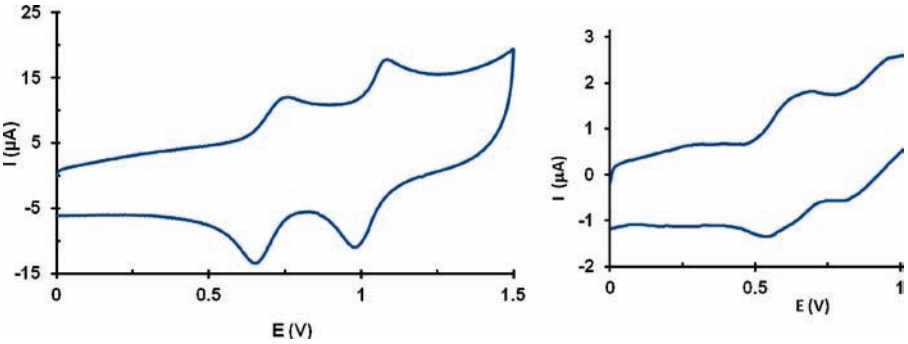

Figure 4. Cyclic voltammograms for (left) acetato-bridged complex $\mathbf{10}^{4+}$ in 0.1 M *n*-Bu_4NPF_6 in CH_2Cl_2 at a 300 mV/s scan rate and (right) aqua complex $\mathbf{13}^{6+}$ at pH = 1.0 in a 0.1 M triflic acid aqueous solution at a 100 mV/s scan rate. In both cases, a glassy carbon electrode is used as the working electrode and the potential is measured vs SSCE.

Table 2. Redox Properties for the Complexes Described in the Present Work ($E_{1/2}$ in V and ΔE in mV) and for Related Ru-Hbpp Complexes for Comparative Purposes[a]

	III−II/II−II		III−III/III−II			IV−III/III−III		III−III/III−II		III−II/II−II	
	$E_{1/2}$	ΔE	$E_{1/2}$	ΔE		$E_{1/2}$	ΔE	$E_{1/2}$	ΔE	$E_{1/2}$	ΔE
$\mathbf{1}^{2+}$	0.71	76	1.12	83	$\mathbf{3}^{3+}$	0.88	110	0.65	64	0.59	64
$\mathbf{4}^{2+}$	0.78	84	1.23	78	$\mathbf{6}^{3+}$	0.90	84	0.65	64	0.56	60
$\mathbf{7}^{4+}$	0.76	82	1.12	123	$\mathbf{13}^{6+}$	0.90	100	0.68	54	0.56	50
$\mathbf{8}^{4+}$	0.77	82	1.13	71	$\mathbf{14}^{6+}$	0.94	86	0.65	60	0.59	72
$\mathbf{9}^{4+}$	0.74	63	1.11	85	$\mathbf{15}^{6+}$	0.94	65	0.65	55	0.59	57
$\mathbf{2}^{2+}$	0.73	86	1.05	86							
$\mathbf{5}^{2+}$	0.79	96	1.15	102							
$\mathbf{10}^{4+}$	0.76	76	1.07	87							
$\mathbf{11}^{4+}$	0.72	67	1.01	104							
$\mathbf{12}^{4+}$	0.73	72	1.03	96							

[a] Chloro- and acetato-bridged complexes are recorded using CH_2Cl_2 as the solvent, whereas the aqua complexes are reported at pH = 1.0 in a 0.1 M triflic acid aqueous solution.

as indicated in the following equation:

$$\{[Ru^{III}Ru^{II}(trpy)_2(\mu\text{-}Cl)]_2(\mu\text{-}(bpp)_2\text{-}p\text{-}xyl)\}^{8+} + 2e^- \rightarrow \{[Ru^{III}Ru^{II}(trpy)_2(\mu\text{-}Cl)]_2(\mu\text{-}(bpp)_2\text{-}p\text{-}xyl)\}^{6+} \quad (3)$$

The 310 mV difference is indicative of relatively strong electronic coupling between the metal centers through the bridging ligands of each subunit. As can be observed in Table 2, complexes $\mathbf{4}^{2+}$ and $\mathbf{5}^{2+}$ containing the bpp-bz$^-$ ligand have significantly higher redox potentials than their bpp$^-$ counterparts $\mathbf{1}^{2+}$ and $\mathbf{2}^{2+}$, as expected because of the electron-withdrawing nature of the benzyl unit. This electronic effect is manifested in both redox processes but to a much larger extent in the second oxidation process. For the III−II/II−II couple, the potentials increase roughly 60−70 mV, whereas for the second one, they increase by 100−110 mV. For the Cl$^-$ and AcO$^-$ tetranuclear complexes, the effect of the benzyl group on the first couple is also observed, although somewhat attenuated. In sharp contrast for the second redox couple, the tetranuclear Cl$^-$ complexes are practically not affected, whereas for the AcO$^-$ ones, the potentials are lower (Table 2). These observations manifest how subtle ligand variations can strongly influence the electronic nature of the species and put forward the difficulty of predicting electronic effects in species resulting from multiple electron-transfer (ET) processes.

The electrochemical properties of the aqua complexes $\mathbf{6}^{3+}$ and $\mathbf{13}^{6+}$−$\mathbf{15}^{6+}$ were also investigated by CV techniques in aqueous solutions, and the voltammograms are shown in Figure 4. The range of pH studied was from 1.0 to 12.0. For complexes $\mathbf{6}^{3+}$ and $\mathbf{13}^{6+}$−$\mathbf{15}^{6+}$, the presence of aqua groups enables proton-coupled ET processes,[27] which occur at relatively low and narrow potentials. The easy access to higher oxidation states is due to the fact that the simultaneous removal of electrons and protons does not allow the buildup of high Coulombic charges in the complex and also due to the σ- and π-donor nature of the oxido group to ruthenium. For complex $\mathbf{13}^{6+}$ at pH = 1, three redox processes are clearly observed and are assigned to the following reactions:

$$[Ru^{III}(OH)\text{-}Ru^{II}(H_2O)]_2^{6+} + 2e^- \rightarrow [Ru^{II}(OH)\text{-}Ru^{II}(H_2O)]_2^{4+} \quad E_{1/2} = 0.33\ V \quad (4)$$

For clarity purposes, only the groups potentially undergoing proton transfer (PT) or ET are written; thus, for instance, $[Ru^{II}(H_2O)\text{-}Ru^{II}(H_2O)]_2^{6+}$ corresponds to complex $\mathbf{13}^{6+}$. Two more redox processes are seen, corresponding to the following equations:

$$[Ru^{III}(OH)\text{-}Ru^{III}(OH)]_2^{6+} + 2e^- + 2H^+ \rightarrow [Ru^{III}(OH)\text{-}Ru^{II}(H_2O)]_2^{6+} \quad E_{1/2} = 0.45\ V \quad (5)$$

dx.doi.org/10.1021/ic101802y |*Inorg. Chem.* 2011, 50, 2771–2781

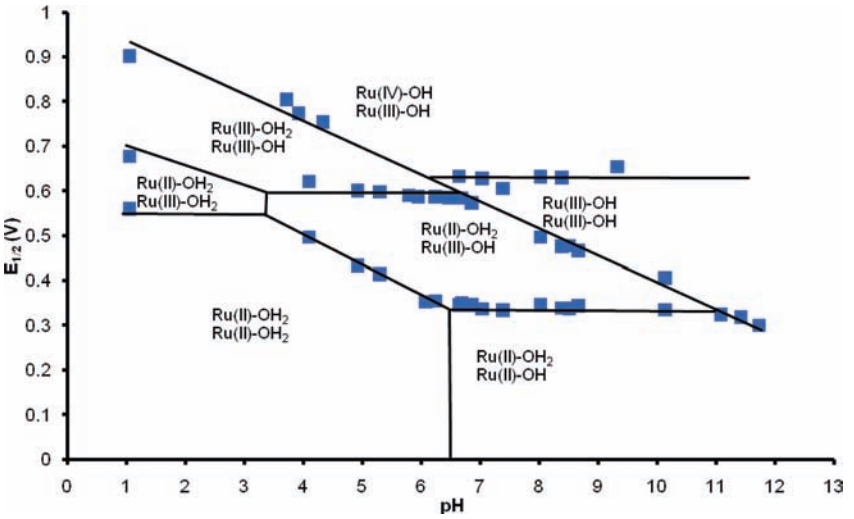

Figure 5. Pourbaix diagram for the aqua complex $\mathbf{13}^{6+}$. The zones of stability of the different species as a function of the pH and $E_{1/2}$ are shown and are indicated by the oxidation state of the ruthenium metal and the degree of protonation of the initial aqua group. For instance, the label [Ru(II)-H_2O Ru(III)OH] is used for $\{[Ru^{II}Ru^{III}(H_2O)(OH)(trpy)_2]_2[(\mu\text{-bpp})_2\text{-}p\text{-xyl}]\}^{6+}$.

$$[Ru^{IV}(OH)\text{-}Ru^{III}(OH)]_2^{8+} + 2e^- \rightarrow [Ru^{III}(OH)\text{-}Ru^{III}(OH)]_2^{6+} \quad E_{1/2} = 0.60\ V \qquad (6)$$

The redox assignment has been carried out by comparison with the parent analogue Ru-Hbpp, $\mathbf{3}^{3+}$, under the same conditions as those reported earlier by us.[10a] The next redox process, which is not observed in the voltammogram, generates the dioxido species $Ru^{IV}(O)$-$Ru^{IV}(O)$, which are proposed to be responsible for the generation of molecular oxygen. As was also the case in the NMR, here the redox behaviors of the two dimeric subunits of the tetranuclear complexes are indistinguishable, manifesting again negligible electronic coupling. The Pourbaix diagram for this complex is represented in Figure 5, indicating the different zones of stability of the corresponding species with a different degree of protonation and/or oxidation. In general, the redox potentials of complexes $\mathbf{6}^{3+}$ and $\mathbf{13}^{6+}$−$\mathbf{15}^{6+}$ are a few millivolts lower than that of $\mathbf{3}^{3+}$, as can be seen in Table 3, because of the electron-withdrawing nature of the benzyl group.

Oxidative Catalysis. The aqua complexes $\mathbf{6}^{3+}$ and $\mathbf{13}^{6+}$−$\mathbf{15}^{6+}$ were tested with regard to their capacity to catalytically oxidize water to molecular oxygen upon the addition of a strong oxidant such as cerium(IV). The evolution of gases was monitored by both manometry and online MS. In the MS experiment, the generated gases were removed from the reaction vessel toward the MS chamber. These results are shown in Figure 6 and Table 3. In all complexes tested in this work, a mixture of O_2 and CO_2 was obtained in sharp contrast with Ru-Hbpp, $\mathbf{3}^{3+}$, where no CO_2 is formed. As a consequence of this, all efficiencies of the complexes reported here are lower than that of $\mathbf{3}^{3+}$. As an example, for the case of $\mathbf{13}^{6+}$ (entry 3, Table 3), the system 1 mM Cat/200 mM Ce/0.1 M triflic acid with a total volume of 2 mL at 25.0 °C gives 20.4 μmol of O_2 and 10.2 μmol of CO_2. These represent turnover numbers (TNs) of 10.1 for O_2 and 5.1 for CO_2. The MS monitoring for this system is displayed in Figure 6b and shows that the O_2 rate of formation is 2 times faster than the CO_2 one. The latter is formed from the very beginning, and thus points to two competitive reactions. An interesting effect is observed when the same system is diluted by half, as shown in entry 4, Table 3. In this case, the total TN significantly increases from 15.2 to 20.7, but the amount of O_2 increases more than the amount of CO_2, and thus the ratio of O_2/CO_2 (r_{o-c}) increases from 2.0 to 2.5. The same phenomenon but to a different extent is observed also for the other two tetranuclear complexes, as can be observed in Table 3 in entries 5−8. This phenomenon can be understood assuming that in the tetranuclear complexes oxygen is formed in an intramolecular manner, in each electronically independent dinuclear subunit, as is the case for the Ru-Hbpp complex $\mathbf{3}^{3+}$.[10c] On the other hand, the origin of CO_2 is associated with a bimolecular reaction where oxidation of the methylenic group of the xylylic bridging unit is attacked by an active Ru−O group of another molecule of $\mathbf{13}^{6+}$. This is the only possible pathway because cerium(IV) does not react with the free ligand at room temperature and the geometrical disposition of the Ru−O units prevents an intramolecular ligand oxidation.[16] Thus, the dilution does not affect the intramolecular O_2 generation reaction but decreases the rate at which CO_2 is generated. The same dilution behavior is also observed for the other two tetranuclear complexes, as displayed in Table 3. Another interesting aspect that can be glimpsed in Table 3 is the fact that for the para and

Table 3. Catalytic Oxidative Performance of Aqua Complexes $\mathbf{6}^{3+}$ and $\mathbf{13}^{6+}$−$\mathbf{15}^{6+}$, Together with $\mathbf{3}^{3+}$ for Comparison Purposes[a]

entry	complex	[Cat]	TN/O_2	TN/CO_2	[O_2]/[CO_2]	TN/total	eff.
1	$\mathbf{3}^{3+}$ [b]	1.0	18				72.0
2	$\mathbf{6}^{3+}$ [b]	1.0	5.8	5.8	1.0	11.7	29.2
3	$\mathbf{13}^{6+}$ [c]	1.0	10.1	5.1	2.0	15.2	33.5
4		0.5	14.8	5.8	2.5	20.7	46.3
5	$\mathbf{14}^{6+}$ [c]	1.0	13.5	6.4	2.1	19.9	45.5
6		0.5	15.6	6.2	2.5	21.9	48.9
7	$\mathbf{15}^{6+}$ [c]	1.0	13.9	6.9	2.0	20.8	46.7
8		0.5	18.4	6.1	3.0	24.5	36.0

[a] All reactions were carried out in a total volume of 2 mL at pH = 1.0 in 0.1 M triflic acid. Cerium(IV) was used as the oxidant. [b] Ratio 1:100 Cat/Ce^{IV}. [c] Ratio 1:200 Cat/Ce^{IV}.

dx.doi.org/10.1021/ic101802y |*Inorg. Chem.* 2011, 50, 2771–2781

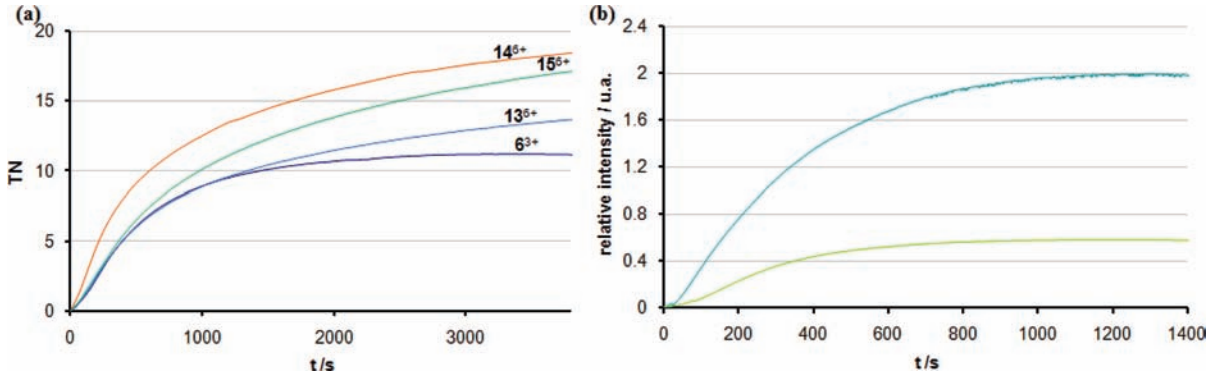

Figure 6. Monitoring of the catalytic gases generated upon the oxidative treatment of 1 mM $\mathbf{6}^{3+}$ and $\mathbf{13}^{6+}-\mathbf{15}^{6+}$ in a pH = 1.0 solution of 0.1 M triflic acid with 100 mM cerium(IV) as a function of time: (a) manometry profile; (b) online MS profile for $\mathbf{15}^{6+}$. Color code: O_2, dark green; CO_2, light green.

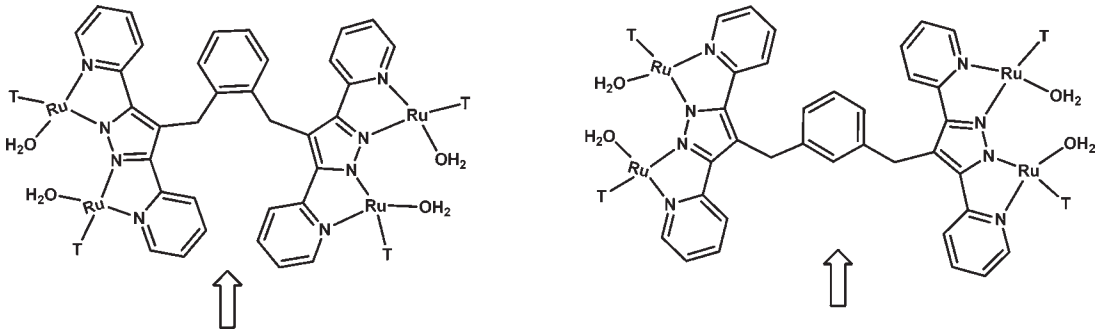

Figure 7. Schematic drawings of complexes $\mathbf{14}^{6+}$ and $\mathbf{15}^{6+}$. The arrows indicate the relative accessibility of the methylenic units for bimolecular oxidation. The trpy ligands are represented by a "T" for clarity purposes, and their axial coordination is not shown.

meta derivatives r_{o-c} increases from roughly 2 to 2.5 when diluting by half. However, for the ortho complex, the same dilution produces a larger increase from 2.0 to 3.0. This larger increase can be associated with the steric accessibility of the methylenic units of the xylylic groups as a function of the geometrical substitution because the methylenic units are the most easily oxidizable groups of the molecule and thus can be assumed as the starting reaction of a chain of the oxidative process. Thus, for the para and meta isomers, the accessibilities of the CH_2 units for the bimolecular reaction are relatively similar, whereas for the ortho isomers, it is significantly restricted, as can be seen in the drawing presented in Figure 7. This is also in agreement with the performance of the dinuclear complex $\mathbf{6}^{3+}$, which has the lowest r_{o-c} value because the steric hindrance in this case is the lowest and, as a consequence, also possesses the lowest efficiency. As mentioned earlier, we associate the formation of CO_2 with oxidation of the benzylic site because this is the easiest part of the molecule to oxidize. Furthermore, once this group is oxidized, the oxidative process does not necessarily stop here and other parts of the already oxidized complex can suffer further oxidative reactions. This type of reactivity had previously been found for a related dinuclear complex attached at the surface of an electrode.[16]

Final Comments and Conclusions. The preparation of a family of tetranuclear ruthenium complexes together with its dinuclear homologue is described. The tetranuclear complexes are made of two subunits containing the bpp^- ligand linked by a xylyl moiety. The pyrazolate moiety of the bpp^- ligand acts as a bridging ligand, providing a relatively intense electronic coupling through the Ru centers of each bpp^- subunit. On the other hand, the Ru centers accommodated in the two subunits do not display any electronic coupling through the xylylic spacer. As a consequence, the spectroscopic and redox properties of the tetranuclear complexes are very similar to those of the dinuclear complex described in the present work. In sharp contrast, the catalytic performances of the four aqua complexes are significantly different. Upon excess cerium(IV), all of the aqua complexes oxidize water to O_2 and generate CO_2. The relative ratio of $[O_2]/[CO_2]$ is dependent on the nature of the complexes because of the fact that water oxidation is an intramolecular process whereas CO_2 generation starts as a bimolecular oxidation process. The latter is significantly different for each of the four aqua complexes described here and can be understood in terms of the accessibility of the easy oxidizable methylenic units of each complex. As a consequence of this, the easiness of oxidizability for the units is $\mathbf{6}^{3+}$ (dinuclear) > $\mathbf{13}^{6+}$ (p) = $\mathbf{14}^{6+}$ (m) > $\mathbf{15}^{6+}$ (o). Thus, in the present case, the performance of the tetranuclear Ru-Hbpp complexes can be understood in terms of the available decomposition pathways.

■ ASSOCIATED CONTENT

Supporting Information. CIF files and further spectroscopic (1D and 2D NMR) details for the reported complexes. This material is available free of charge via the Internet at http://pubs.acs.org. The supplementary crystallographic data can also be obtained free of charge via www.ccdc.cam.ac.uk/conts/retrieving.html (or from the Cambridge Crystallographic Data Centre, 12 Union Road, Cambridge CB2 1EZ, U.K.; fax +44 1223 336033 or e-mail deposit@ccdc.cam.ac.uk).

dx.doi.org/10.1021/ic101802y |*Inorg. Chem.* 2011, 50, 2771–2781

AUTHOR INFORMATION

Corresponding Author
*E-mail: lluis.escriche@uab.cat (L.E.), allobet@iciq.es (A.L.).

ACKNOWLEDGMENT

Support from SOLAR-H2 (EU 212508) and MEC (CTQ2010-21497 and Consolider Ingenio 2010 CSD2006-0003) is gratefully acknowledged. L.F. is grateful for the award of a doctoral grant from Universitat Autònoma de Barcelona.

REFERENCES

(1) Benniston, A. C.; Harriman, A. *Mater. Today* **2008**, *11*, 26–34.
(2) (a) Sala, X.; Rodriguez, M.; Romero, I.; Escriche, L.; Llobet, A. *Angew. Chem., Int. Ed.* **2009**, *48*, 2842. (b) Romain, S.; Vigara, L.; Llobet, A. *Acc. Chem. Res.* **2009**, *42*, 1944–1953. (c) Sartorel, A.; Miró, A.; Salvadori, E.; Romain, S.; Carraro, M.; Scorrano, G.; Di Valentin, M.; Llobet, A.; Bo, C.; Bonchio, M. *J. Am. Chem. Soc.* **2009**, *131*, 1651–1653. (d) Sartorel, A.; Carraro, M.; Scorrano, G.; De Zorzi, R.; Geremia, S.; McDaniel, N. D.; Bernhard, S.; Bonchio, M. *J. Am. Chem. Soc.* **2008**, *130*, 5006. (e) Puntoriero, F.; La Ganga, G.; Sartorel, A.; Carraro, M.; Scorrano, G.; Bonchio, M.; Campagna, S. *Chem. Commun.* **2010**, *46*, 4725–4727. (f) Geletii, Y. V.; Botar, B.; Koegler, P.; Hillesheim, D. A.; Musaev, D. G.; Hill, C. L. *Angew. Chem., Int. Ed.* **2008**, *47*, 3896–3899. (g) Geletii, Y. V.; Huang, Z.; Hou, Y.; Musaev, D. G.; Lian, T.; Hill, C. L. *J. Am. Chem. Soc.* **2009**, *131*, 7522–7523.
(3) (a) Gilbert, J. A.; Eggleston, D. S.; Murphy, W. R.; Geselowitz, D. A.; Gersten, S. W.; Hodgson, D. J.; Meyer, T. J. *J. Am. Chem. Soc.* **1985**, *107*, 3855–3864. (b) Concepcion, J.; Jurss, J. W.; Templeton, J. L.; Meyer, T. J. *J. Am. Chem. Soc.* **2008**, *130*, 16462–16463. (c) Zhang, G.; Zong, R.; Tseng, H. W.; Thummel, R. P. *Inorg. Chem.* **2008**, *47*, 990–998.
(4) (a) Alstrum-Acevedo, J. H.; Brennaman, M. K.; Meyer, T. J. *Inorg. Chem.* **2005**, *44*, 6802–6827. (b) Magnuson, A.; Anderlund, M.; Johansson, O.; Lindblad, P.; Lomoth, R.; Polivka, T.; Ott, S.; Stensjo, K.; Styring, S.; Sundstrom, V.; Hammarstrom, L. *Acc. Chem. Res.* **2009**, *42*, 1899–1909. (c) Concepcion, J. J.; Jurss, J. W.; Brennaman, M. K.; Hoertz, P. G.; Patrocinio, A. O. T.; Iha, N. Y. M.; Templeton, J. L.; Meyer, T. J. *Acc. Chem. Res.* **2009**, *42*, 1954–1965. (d) Youngblood, W. J.; Lee, S. H.-A.; Maeda, K.; Mallouk, T. E. *Acc. Chem. Res.* **2009**, *42*, 1966–1973.
(5) (a) Hull, J. F.; Balcells, D.; Blakemore, J. D.; Incarvito, C. D.; Eisenstein, O.; Brudvig, G. W.; Crabtree, R. H. *J. Am. Chem. Soc.* **2009**, *131*, 8730–8731. (b) McDaniel, N. D.; Coughlin, F. J.; Tinker, L. L.; Bernhard, S. *J. Am. Chem. Soc.* **2008**, *130*, 210–217.
(6) (a) Kanan, M. W.; Nocera, D. G. *Science* **2008**, *321*, 1072. (b) Lutterman, D. A.; Surendranath, Y.; Nocera, D. G. *J. Am. Chem. Soc.* **2009**, *131*, 3838–3839. (c) Surendranath, Y.; Dinca, M.; Nocera, D. G. *J. Am. Chem. Soc.* **2009**, *131*, 2615–2620. (d) Yin, Q.; Tan, J. M.; Besson, C.; Geletii, Y. V.; Musaev, D. G.; Kuznetsov, A. E.; Luo, Z.; Hardcastle, K. I.; Hill, C. L. *Science* **2010**, *328*, 342–345.
(7) Ellis, W. C.; McDaniel, N. D.; Bernhard, S.; Collins, T. J. *J. Am. Chem. Soc.* **2010**, *132*, 10990–10991.
(8) Chen, J.; Faller, J. W.; Crabtree, R. H.; Brudvig, G. W. *J. Am. Chem. Soc.* **2004**, *126*, 7345–7349.
(9) (a) Yano, J.; Kern, J.; Sauer, K.; Latimer, M. J.; Pushkar, Y.; Biesiadka, J.; Loll, B.; Saenger, W.; Messinger, J.; Zouni, A.; Yachandra, V. K. *Science* **2006**, *314*, 821. (b) Haumann, M.; Liebisch, P.; Müller, C.; Barra, M.; Grabolle, M.; Dau, H. *Science* **2005**, *310*, 1019.
(10) (a) Sens, C.; Romero, I.; Rodríguez, M.; Llobet, A.; Parella, T.; Benet-Buccholz, J. *J. Am. Chem. Soc.* **2004**, *126*, 7798–7799. (b) Mola, J.; Mas-Marzá, E.; Sala, X.; Romero, I.; Rodríguez, M.; Viñas, C.; Parella, T.; Llobet, A. *Angew. Chem., Int. Ed.* **2008**, *47*, 5830–5832. (c) Romain, S.; Bozoglian, F.; Sala, X.; Llobet, A. *J. Am. Chem. Soc.* **2009**, *131*, 2768.
(11) Bozoglian, F.; Romain, S.; Ertem, M. Z.; Todorova, T. K.; Sens, C.; Mola, J.; Rodríguez, M.; Romero, I.; Benet-Buchholz, J.; Fontrodona, X.; Cramer, C. J.; Gagliardi, L.; Llobet, A. *J. Am. Chem. Soc.* **2009**, *131*, 15176–15187.
(12) Concepcion, J. J.; Jurss, J. W.; Templeton, J. L.; Meyer, T. J. *J. Am. Chem. Soc.* **2008**, *130*, 16462–16463.
(13) (a) Wasylenko, D. J.; Ganesamoorthy, C.; Koivisto, B. D.; Henderson, M. A.; Berlinguette, C. P. *Inorg. Chem.* **2010**, *49*, 2202–2209. (b) Wasylenko, D. J.; Ganesamoorthy, C.; Koivisto, B. D.; Berlinguette, C. P. *Eur. J. Inorg. Chem.* **2010**, *20*, 315–342.
(14) Masaoka, S.; Sakai, K. *Chem. Lett.* **2009**, *38*, 182–183.
(15) Teixidor, F.; Garcia, R.; Pons, J.; Casabó, J. *Polyhedron* **1988**, *7*, 43.
(16) Francàs, L.; Sala, X.; Benet-Buchholz, J.; Escriche, L.; Llobet, A. *ChemSusChem* **2009**, *2*, 321–329.
(17) Sullivan, B. P.; Calvert, J. M.; Meyer, T. J. *Inorg. Chem.* **1980**, *19*, 1404.
(18) Data collection with: *APEX II*, versions v1.0-22, v2009.1-0, and v2009.1-02; Bruker AXS Inc.: Madison, WI, 2007.
(19) Data reduction with: *SAINT*, versions V.2.10 (2003), V/.60A, and V7.60A; Bruker AXS Inc.: Madison, WI, 2007.
(20) *SADABS*, versions V.2.10 (2003); V2008, and V2008/1 (2001); Bruker AXS Inc.: Madison, WI, 2008. Blessing, R. H. *Acta Crystallogr.* **1995**, *A51*, 33–38.
(21) Sheldrick, G. M. *Acta Crystallogr.* **2008**, *A64*, 112−122 (*SHELXTL*, versions V6.12 and V6.14).
(22) *SQUEEZE*: Van der Sluis, P.; Spek, A. L. *Acta Crystallogr.* **1990**, *A46*, 194.
(23) *PLATON*: Spek, A. L. *J. Appl. Crystallogr.* **2003**, *36*, 7–13.
(24) (a) Laurent, F.; Plantalech, E.; Donnadieu, B.; Jimenez, A.; Hernandez, F.; Martinez-Ripoll, M.; Biner, M.; Llobet, A. *Polyhedron* **1999**, *18*, 3321. (b) Romero, I.; Rodriguez, M.; Llobet, A.; Collomb-Dunand-Sauthier, M.-N.; Deronzier, A.; Parella, T.; Soteckli-Evans, H. *J. Chem. Soc., Dalton Trans.* **2000**, 1689. (c) Sens, C.; Rodriguez, M.; Romero, I.; Llobet, A.; Parella, T.; Benet-Buchholz, J. *Inorg. Chem.* **2003**, *42*, 8385. (d) Sala, X.; Romero, I.; Rodriguez, M.; Llobet, A.; Gonzalez, G.; Martinez, M.; Benet-Buchholz, J. *Inorg. Chem.* **2004**, *43*, 5403. (e) Sala, X.; Plantalech, E.; Poater, A.; Rodriguez, M.; Romero, I.; Sola, M.; Llobet, A.; Jansat, S.; Gómez, M.; Stoeckli-Evans, H.; Benet-Buchholz, J. *Chem.—Eur. J.* **2006**, *12*, 2798.
(25) Planas, N.; Christian, G. J.; Mas-Marzà, E.; Sala, X.; Fontrodona, X.; Maseras, F.; Llobet, A. *Chem.—Eur. J.* **2010**, *16*, 7965–7968.
(26) (a) Haga, M.; Dodsworth, E. S.; Lever, A. B. P. *Inorg. Chem.* **1986**, *25*, 447–453. (b) Rasmussen, S. C.; Ronco, S. E.; Mlsna, D. A.; Billadeau, M. A.; Pennington, W. T.; Kolis, J. W.; Petersen, J. D. *Inorg. Chem.* **1995**, *34*, 821–829. (c) Kohle, O.; Ruile, S.; Gratzel, M. *Inorg. Chem.* **1996**, *35*, 4779–4787. (d) Ben Altabel, A.; Ribotta, S. B.; de Gallo, R.; Folquer, M. E.; Katz, N. E. *Inorg. Chim. Acta* **1991**, *188*, 67–70. (e) Anderson, P. E.; Deacon, G. B.; Haarmann, K. H.; Keene, F. R.; Meyer, T. J.; Reitsma, D. A.; Skelton, B. W.; Strouse, G. F.; Thomas, N. C.; Treadway, T. A.; White, T. A. *Inorg. Chem.* **1995**, *34*, 6145–6157. (f) Barqawi, K. R.; Llobet, A.; Meyer, T. J. *J. Am. Chem. Soc.* **1988**, *110*, 7751–7759.
(27) Huynh, M. H. V.; Meyer, T. J. *Chem. Rev.* **2007**, *107*, 5004–5064.

NOTE ADDED AFTER ASAP PUBLICATION

This paper was published on the Web on March 2, 2011. Due to a production error, the element cerium(IV) was incorrectly identified throughout the article as cesium(IV). The corrected version was reposted on March 21, 2011.